Chapter 3

Experience with Water Balance, Evapotranspiration, and Predictions of Water Stress Effects in the CROPGRO Model

K. J. Boote
Agronomy Department, University of Florida, Gainesville

Federico Sau
Departamento de Biologia Vegetal, Universidad Politecnica de Madrid, Spain

Gerrit Hoogenboom
Dep. of Biological and Agricultural Engineering, University of Georgia, Griffin

James W. Jones
Agricultural and Biological Engineering Dep., University of Florida, Gainesville

Abstract

Crop models should accurately predict soil water balance, evapotranspiration (ET), and water deficit effects on growth and development processes and ultimately yield. We (i) describe the soil water balance and ET options in the CROPGRO model; (ii) illustrate how water stress effects are implemented on processes of photosynthesis–transpiration, leaf expansion, internode elongation, assimilate partitioning, pod addition, vegetative node expression, and reproductive development; (iii) document the dynamic growth responses of the CROPGRO model to water deficit; (iv) highlight tests of soil water balance and ET that justify recent changes and future needed improvements; and (v) explore new ways of modeling crop perception of water deficit that translate into better prediction of responses observed in literature. We conclude the Ritchie tipping bucket soil water balance model in DSSAT (Decision Support System for Agrotechnology Transfer software; Jones et al., 2003) generally works satisfactorily when the soil water-holding traits (drained upper limit, DUL; lower limit of plant-extractable soil water, LL) are estimated properly and when root growth is adequately predicted. Of the potential evapotranspiration (PET) options, the Priestley-Taylor option is the default because it does not require windrun or dewpoint. We find the Priestley-Taylor option predicts ET satisfactorily when the extinction coefficient (total solar energy extinction coefficient, KEP) for partitioning PET to transpiration is reduced from 0.85 to 0.70 for all CROPGRO V4.0 crops and from 1.00 to 0.68 for CERES-Maize. When windrun and dewpoint are available, then the FAO-56 PET option is generally best, while the FAO-24 PET option overpredicts ET. Where the soil water balance is adequately predicted, the crop water stress signals, soil water stress factor (SWFAC), and plant turgor factor (TURFAC) appear to function well to modify crop assimilation, expansive growth processes, and crop development. Simulated comparisons with field data illustrate how these signals act to enhance partitioning to root, reduce leaf area, and accelerate crop maturity. Overall, CROPGRO satisfactorily simulates water deficit effects on growth and development processes, although crop-specific signals that act sooner than the current TURFAC are needed to accelerate or delay the onset of reproductive growth.

Response of crops to limited water: Understanding and modeling water stress effects on plant growth processes.
Advances in Agricultural Systems Modeling Series 1.

David Drexler

The CSM-CROPGRO models, along with the CERES models, are part of the DSSAT V4.0 (Decision Support System for Agrotechnology Transfer) software (Jones et al., 2003). The CSM-CROPGRO model is a process-oriented, mechanistic model with subroutines that simulate crop development, C balance, crop and soil N balance, and soil water balance, which have been described in detail by Boote et al. (1998a, 1998b). Crop development includes vegetative and reproductive development processes that determine life cycle duration, duration of root and leaf growth, and onset and duration of reproductive organ growth. Thus, crop development influences dry matter partitioning among plant organs over time. The crop C balance includes daily inputs from photosynthesis, conversion of C into crop tissue growth, C losses through abscission, and maintenance respiration. The C balance also includes leaf area expansion, growth of vegetative tissues, pod addition, seed addition, shell growth, seed growth, nodule growth, tissue senescence, and carbohydrate mobilization. The crop N balance includes daily soil N uptake, N_2 fixation, mobilization and translocation of N from old vegetative tissues to growth of new vegetative or reproductive tissues, rate of N use for new tissue growth, and rate of N loss in abscised parts. Soil N balance processes are those described by Godwin and Jones (1991) and Godwin and Singh (1998). The time step in CROPGRO is mostly daily for C, N, and water balance processes, but is hourly for some processes, such as calculation of thermal time and scaling of leaf to canopy assimilation. The time step for soil water balance and ET is daily, and matches the timing of weather data input and daily dry matter growth (Ritchie, 1998). Model state variables are predicted and output on a daily basis for crop, soil water, and soil N balance processes.

CSM-CROPGRO is a generic model that uses one common FORTRAN code to predict the growth of more than seven different grain legumes as well as several nonlegumes (Hoogenboom et al., 1991, 1992, 1993; Boote et al., 1998a, 1998b; Jones et al., 2003). This versatility is achieved by abstracting the plant processes to a common level such that only differences in parameters are needed to simulate a range of crops. These parameters are species traits and cultivar attributes that are defined and read in as input files. The species file includes partitioning coefficients, tissue compositions, conversion costs, photosynthesis sensitivity to leaf N, relationships to water stresses, and cardinal temperature sensitivities for

processes such as photosynthesis, nodule growth, N_2 fixation, maintenance respiration, leaf area growth, pod addition, and seed growth. The model code along with information input from the species, ecotype, and cultivar files is based on understanding of crop–soil–weather relationships. More information on CROPGRO's generic nature and file input structure is available (Hoogenboom et al., 1994; Boote et al., 1998a, 1998b; Boote et al., 2004; Jones et al., 2004; Porter et al., 2004). The CROPGRO model originated from the SOYGRO 4.2 developed by Wilkerson et al. (1983). Between 1989 and 1994, major model innovation occurred; the soil N balance and N uptake features as well as N fixation were added, resulting in the release of the first version of CROPGRO V3.0 in 1994 (Hoogenboom et al., 1991, 1992, 1993), then Version 3.1 in 1996, Version 3.5 in 1998, Version 4.0 in 2004, and Version 4.02 in 2005. Since 2004, the models have included two options for soil organic matter: the default "Godwin" version (Godwin and Singh, 1998), or the "Parton" CENTURY version that was linked by Gijsman et al. (2002a). In this release of the Cropping System Model (CSM) in the DSSAT V4.0 (Jones et al., 2003), the CROPGRO and CERES models share the same soil water and soil N balances as a true land unit module and have carryover of soil water, soil N, and organic C that facilitates long-term sequence–rotation studies.

Processes Related to Water Balance in CROPGRO

Soil Water Balance in CROPGRO

The CROPGRO and CERES models use the one-dimensional tipping bucket soil water balance described by Ritchie (1985, 1998) and by Porter et al. (2004). Soil water balance processes include infiltration of rainfall and irrigation, runoff, soil evaporation, crop transpiration, distribution of root water uptake from soil layers, and drainage of water through the profile and below the root zone. The soil is divided into a number of computational layers, up to a maximum of 20. Water content in each layer varies between the lower limit of plant extractable soil water [LL(J)], the drained upper limit [DUL(J)], and the saturated soil water content [SAT(J)]. If water content of a given layer is above the DUL, then water is drained to the next layer with the "tipping bucket" approach, using a profile-wide drainage coefficient (SWCON). If available, saturated hydraulic conductivity (K_{sat}) for water flow of each specific soil layer can be entered to control vertical drainage from one layer to the next. This feature allows the soil to retain water above the DUL for layers that have sufficiently low K_{sat} for water flow, and in this case, soil layers may become saturated for sufficient time to cause root death, reduced root water uptake, anoxia-induced stress, and decreased N fixation. Water between SAT and DUL is available for root uptake subject to the anoxia-induced problem

that is triggered when air-filled pore space falls below 2% of total volumetric pore space. Infiltration and runoff of rainfall and applied irrigation water depends on the Soil Conservation Service runoff curve number. Soil evaporation and transpiration are described below. The DSSAT V4 software includes a pedotransfer function (SBUILD) that computes the LL, DUL, and SAT, derived from sand, silt, clay, soil organic C content, and bulk density. The pedotransfer function is based mostly on the Saxton et al. (1986) method as described by Gijsman et al. (2002b).

Evapotranspiration Options

The CROPGRO and CERES models have three options for computing climatic potential evapotranspiration (PET, equivalent to ET_o): (i) Priestley-Taylor method (Priestley and Taylor, 1972) also described by Ritchie (1985), (ii) FAO-Penman-24 method described by Jensen et al. (1990), and (iii) the FAO-56 described by Allen et al. (1998) as implemented in CROPGRO by Sau et al. (2004). CROPGRO, additionally, has an hourly three-zone energy balance option (Pickering et al., 1995) that is still in research mode and needs improvement for convection terms for incomplete canopies where it predicts unrealistically high foliage temperatures. The default PET option is the Priestley-Taylor option, primarily because it is the less demanding of weather data (it is the only one that does not require daily windspeed or dewpoint temperature as input). The other methods additionally require wind speed and humidity (actually dewpoint temperature). We recommend the FAO-56 over the FAO-24 method, as the FAO-Penman-24 overpredicts ET and predicts too much plant stress (Allen et al., 1998; Sau et al., 2004).

While the first three PET options are widely used and described, more explanation is needed for the hourly ET and three-zone energy balance option (ETPHOT). The latter ET option was incorporated into the CROPGRO model by Pickering et al. (1995) to enhance model responsiveness to climate change factors. The hourly energy balance version uses hourly solar radiation, air temperature, humidity, and windspeed as inputs, and is linked to the hedgerow canopy assimilation model of Boote and Pickering (1994) that predicts leaf photosynthesis and stomatal conductance of sunlit and shaded leaf classes and integrates to canopy assimilation. The hourly energy balance option (Pickering et al., 1990, 1995) solves for rate of water loss and temperature of three zones: sunlit leaves, shaded leaves, and soil surface, using a matrix inversion approach patterned after Jagtap and Jones (1989). The hedgerow canopy assimilation model of Boote and Pickering (1994) requires inputs of latitude, row spacing, spacing between plants in the row, row direction, leaf angle distribution, leaf width, radiation scattering coefficients, and leaf photosynthesis traits (potential light-saturated leaf photosynthesis, quantum efficiency, leaf respiration, and cuticular resistance). The crop

model dynamically predicts canopy height, canopy width, and leaf area index (LAI). The hedgerow light absorption approach was patterned after Gijzen and Goudriaan (1989) with modifications described by Boote and Pickering (1994)) where individual plants are ellipsoids defined by height and width and cast elliptical shadows as affected by row spacing, plant spacing, row azimuth, day-of-year, time-of-day, and latitude. The ET module uses the same radiation absorption submodel as for photosynthesis, except for a second pass through the radiation absorption submodel for nonphotosynthetically active irradiance with different scattering coefficients.

Stomatal conductance is computed from leaf assimilation with assumption of constant ratio of intercellular to ambient CO_2 (C_i/C_a) above the CO_2 compensation point (Pickering et al., 1995). The ETPHOT module additionally requires root water uptake parameters and soil parameters (layer thickness, DUL, LL, bulk density, reflectivity, first-stage evaporation limit, number of evaporation layers, dry thermal capacity and conductivity). Some variables change daily during the season to include day-of-year, daily meteorological variables, daily soil water variables (infiltration, soil water content, and root length density distribution with depth), canopy architecture (height, width, and LAI predicted by the crop model), and leaf photosynthesis parameters (leaf N concentration and specific leaf area predicted by the crop model). ETPHOT will run with standard Class A weather data [solar radiation; T_{max}, daily maximum air temperature; T_{min}, daily minimum air temperature; rainfall] plus CO_2 concentration. Actual dewpoint is preferred, otherwise the default for dewpoint temperature is assumed to be equal to the $T_{\min}$. Daily wind speed is desirable, but otherwise a default daily windrun is assumed. CROPGRO computes hourly weather data from daily inputs. A full-sine wave is used to compute the hourly radiation values from daily solar radiation integral and daylength. A combined sine-exponential curve (Parton and Logan, 1981; Kimball and Bellamy, 1986) is used to predict hourly air temperatures from $T_{\max}$ and $T_{\min}$. Hourly total and photosynthetic irradiance are separated into direct and diffuse components using a fraction diffuse vs. atmospheric transmission algorithm (Erbs et al., 1982; Spitters et al., 1986).

The ETPHOT model computes the absorption of direct and diffuse irradiance by sunlit and shaded leaf classes two times; once for the photosynthetically active irradiance using appropriate scattering and extinction coefficients, and then a second time with the nonphotosynthetic irradiance (mostly infrared) using a different set of scattering and extinction coefficients. The irradiance not absorbed by the foliage is transmitted to the soil, but also subject to reflectance toward the foliage in the above absorptance submodel. Using energy absorptance by the three zones (sunlit LAI, shaded LAI, and soil surface) as described in Fig. 4–3 of Picker-

ing et al. (1995), the equations for the energy balance predict sensible and latent fluxes from each zone to a fully mixed canopy following the approach of Jagtap and Jones (1989). This system of 11 equations contains 12 unknowns, but the temperature of the first soil layer from the previous time step is used to construct an additional equation for the soil heat flux, thus facilitating an exact solution. Under water-limiting conditions, the model goes through several iterations to solve for the sunlit and shaded leaf temperatures, leaf assimilation, and conductance that match the amount of water that roots can supply. Further information is available in Pickering et al. (1995) and Pickering et al. (1990) to include description of computing leaf boundary layer and aerodynamic resistances to heat and vapor loss. Those papers also illustrate ETPHOT predictions of leaf-to-air temperature differential as affected by vapor pressure deficit and predictions of CO_2 effects on ET. The hourly energy balance option is sensitive to CO_2 that partially closes stomata and increases water use efficiency while increasing foliage temperature by about 1°C (Boote et al., 1997). Williams and Boote (1995) also used it to predict that water use efficiency of peanut (*Arachis hypogaea* L.) was enhanced with an increase in specific leaf weight because of lower C_i/C_a ratio.

Partitioning to Plant Transpiration versus Soil Evaporation

The DSSAT crop models partition the PET to potential plant transpiration (EP_O) and potential soil evaporation (ES_O), following the Ritchie (1972, 1985) approach, which considers the portion of net radiation that reaches the soil and that can be spent as latent energy to evaporate water from the soil surface if the soil is wet. The climatic EP_O is computed by multiplying the PET of Options 1, 2, or 3 by the exponential function of LAI shown in Eq. [1] using a KEP that is smaller than the extinction coefficient for photosynthetically active radiation. Energy not absorbed by the crop is transmitted to the soil surface (Eq. [2]) and is available to drive ES_O. Sau et al. (2004) argued that the KEP for total solar energy extinction coefficient should be close to 0.50, which agrees with experimentally measured values of 0.52 (Villalobos and Fereres, 1990) and theoretical values of 0.46 to 0.53 computable from Goudriaan (1977) and Goudriaan and Van Laar (1994). Based on Sau et al. (2004), the KEP for the DSSAT V4 release was lowered from 0.85 to 0.70 and from 1.00 to 0.68, respectively, for the CROPGRO and CERES models. Because of inertia to model change, the extinction coefficient for solar radiation transmittance to the soil surface (Eq. [2]) is presently about 0.4 in the DSSAT models although the value in theory should be the same as KEP.

$$EP_O = PET \times [1.0 - \exp(-KEP \times LAI)] \quad [1]$$

$$ES_O = PET \times \exp(-0.40 \times LAI) \quad [2]$$

The actual soil evaporation (ES) and plant transpiration (EP) depend on the availability of water to meet these potential rates. The current DSSAT models compute the ES following the two-stage soil evaporation method of Ritchie (1985): (i) the energy-limited stage (Stage 1); and (ii) the falling-rate stage (Stage 2) that begins after the first stage loss has been met, after which ES declines as the square root of time. The Stage 1 soil water evaporation limit is a value defined for each soil profile; once this amount is achieved, the evaporation follows the falling-rate stage. In addition, ES is allowed to have access only to the soil water in the top 5 cm of soil (for all soils) that limits the function. The two-stage soil evaporation method is not particularly good, and improvements are being considered for the next DSSAT release. If the potential ES_O energy is not used for ES during Stage 2, it is presumed absorbed by the canopy as follows:

$$\text{IF } EP_O + ES < PET, \text{ THEN } EP_O = PET - ES \quad [3]$$

Root Water Uptake and Water Stress Factors

Root water uptake must be computed before the actual canopy transpiration (EP) is computed. Potential root water uptake per soil layer, RWU(L), is a function of root length density (RLD) and soil water content within each soil layer using a simplified computation of radial flow to roots (Ritchie, 1985) as shown in Eq. [4] where C_1, C_2, and C_3 are constants. The total potential root water uptake (TRWU) is integrated over RWU of root length in all soil layers, TRWU = ∑RWU(L), and is then compared with climatic EP_O. If EP_O is less than TRWU, then actual root water uptake is limited to EP_O (Eq. [5] and [6]). The TRWU is usually larger than EP_O, until the soil water reaches a given level of depletion.

$$RWU(L) = C_1 \times EXP[MIN(\{C_2(L) \times [SW(L) - LL(L)]\},40)]/\{C_3 - ALOG[RLD(L)]\} \quad [4]$$

$$\text{IF } TRWU > EP_O, \text{ THEN } EP = EP_O \quad [5]$$

$$\text{IF } TRWU < EP_O, \text{ THEN } EP = TRWU \quad [6]$$

The ratio of TRWU to EP_O is used to compute water deficit effects, via two different ratios (SWFAC and TURFAC) per Eq. [7] and Eq. [8]. These can be viewed as signals that regulate crop processes. Figure 3–1 shows graphically the meaning of SWFAC and TURFAC. TURFAC and an "early" signal are also computed from TRWU and EP_O, but are scaled by 1.5 or K_1 to act before photosynthesis is reduced. SWDF3 in Eq. [9] is a hypothetical "early" signal with a K_1 ranging from 2.5 to 5.0, and is designed to act sooner than TURFAC or SWFAC. This "early" signal will be discussed in a later section.

$$SWFAC = TRWU/EP_O, \text{ limited to a maximum of 1.0} \quad [7]$$

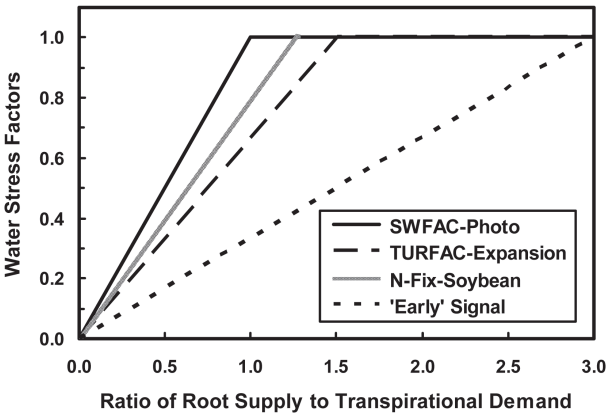

Fig. 3–1. Four water stress signals, SWFAC for photosynthesis, TURFAC for expansive processes, N-Fix-Soybean for nodule growth and nitrogenase activity, and an "early" signal, computed from the ratio of potential root water supply to transpirational demand for water.

$$\text{TURFAC} = \text{TRWU}/(\text{EP}_\text{O} \times 1.5), \text{ limited to a maximum of } 1.0 \quad [8]$$

$$\text{SWDF3} = \text{TRWU}/(\text{EP}_\text{O} \times K1), \text{ limited to a maximum of } 1.0 \quad [9]$$

When the SWFAC (Eq. [7]) is less than 1.0, then daily photosynthesis and transpiration are reduced in a one-to-one manner (proportional to SWFAC). This is a mimic of stomatal action, allowing CO_2 to be fixed in proportion to the stomatal opening to allow for transpiration. CROPGRO has no vapor pressure deficit effect on photosynthesis or stomatal function. When SWFAC is less than 1.0, root depth progression is accelerated, leaf senescence is more rapid, crop phenology may be delayed or accelerated depending on the crop growth phase, and N is mobilized more rapidly during seed fill. When TURFAC (Eq. [8]) is less than 1.0, the expansion of new leaves and internode elongation (height and width increase) are reduced. A TURFAC less than 1.0 reduces rate of leaf appearance (V-stage), specific leaf area of new leaves, the increase in height and width, N fixation, and it shifts allocation from leaf and stem toward root.

Root Growth in CROPGRO

Root mass and root length in each soil layer are model state variables that are computed daily. New root length produced each day depends on daily assimilate allocated to roots and a constant length-to-weight parameter. Fraction partitioning of assimilate to root varies with crop growth stage and eventually becomes zero when reproductive growth uses all the daily assimilate. The distribution of the new RLD into respective layers depends on progress of downward root depth front, a soil-rooting preference function (SRGF) describing the probability of roots growing in each soil layer, and the soil water content of each layer. The SRGF defines the hospitality of the soil (soil impedance, soil pH, soil nutrient effect, and organic matter effect) to root proliferation. Rate of root depth

progression (RTPROG) in Eq. [10] is a function of thermal time accumulation (DTX), a species potential root depth progression rate in centimeters per thermal day (RFAC2), is accelerated as much as 15% by SWFAC, and is dependent on soil water status of the rooting front layer (reduced only when fraction available water is less than 0.25 or reduced if water content is very high, within 2% of saturation). The SWDF(L) in Eq. [10, 11, 12] is not fraction available water and is not SWFAC, rather SWDF(L) = {SW(L) − LL(L)]/(0.25 × [DUL(L) − LL(L)]} and mimics increased soil impedance, occurring when available water in layer *L* is less than 25% of (DUL − LL). SWEXF(L) is anaerobic stress computed from fraction of pore space filled with water for the rooting front layer (*L*). While CROPGRO accelerates root depth with water stress, CERES-Maize is different, and uses SWFAC as a third factor in the MIN part of the equation to limit root depth progression with plant water stress.

$$\text{RTPROG} = \text{DTX} \times \text{RFAC2} \times \text{MIN}[\text{SWDF(L)}, \text{SWEXF(L)}] \times \{1.0 + 0.25 \times [1.0 - \text{MAX}(\text{SWFAC}, 0.40)]\} \quad [10]$$

It is logical that root depth progression into a moist soil layer would actually be accelerated if shoot expansion is restricted, and the soil water content of the rooting front zone is not limiting. This is a feature learned through experience in simulating severe drought situations (1978, Gainesville, FL; 1988, Ames IA; 1981, Gainesville, FL; 1985, Gainesville, FL; and 1991, Potchefstroom, South Africa), where better simulations were obtained when plant water stress accelerated rooting depth progression rather than inhibiting it as the code initially did. With the South Africa data set, the crop was sown on a profile with about half the available water capacity. Because of the drying soil and SWFAC restriction of root depth progression in the old model version, the roots did not grow downward and the simulated crop actually died, whereas the real crop survived. For this reason, the code (Eq. [10]) for root depth increase in CROPGRO V3.5 and V4.0 was changed from one with root depth progression restricted proportional to SWFAC, to one with acceleration with SWFAC. A simulated constitutive (all the time) 10% greater RTPROG was shown to increase soybean (*Glycine max* L.) yield about 2.4% for the Ames, IA, location (Boote et al., 2003); and an adaptive response under plant water deficit would likewise be beneficial. Increased assimilate allocation to root growth is already a feature in the model.

The fraction of new root length increase allocated to a given layer of soil, RLDF(L), is dependent on the Soil Root Growth preference Function [SRGF(L)], layer thickness [DLAYR(L)], the presence of the rooting front in that layer, and the soil water status of that layer [SWDF(L) and SWEXF(L)] defined the same as for

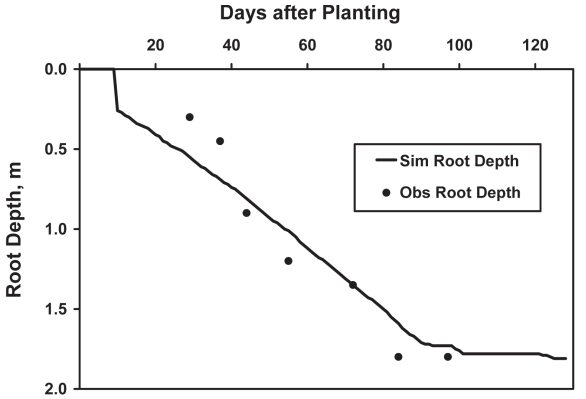

Fig. 3–2. Simulated and observed root depth progression over time for Wayne soybean grown on an Ida silt loam soil at Castana, IA, in 1979 (data from Mason et al., 1980).

root depth progression (Eq. [11]). We assume that roots will grow into a soil layer if its water content is above 25% of (DUL − LL).

$$RLDF(L) = SRGF(L) \times DLAYR(L) \times MIN[SWDF(L), SWEXF(L)] \quad [11]$$

There is senescence of RLD in each layer as a function of thermal time, accelerated when available soil water content is below a critical fraction (0.25) or near saturation. Root senescence is influenced by soil water status and water excess of each soil layer. In Eq. [12], RTSURV is fraction root survival, RTSDF is fraction root death under zero water availability and RTEXF is fraction root death under fully saturated soil.

$$RTSURV(L) = MIN(1.0,\{1.0 - RTSDF \times [1.0 - SWDF(L)]\}, \{1.0 - RTEXF \times [1.0 - SWEXF(L)]\}) \quad [12]$$

In addition, Eq. [13] provides a thermal time dependent rate of root length senescence in each layer, where RTSEN (0.02) is the fraction senesced per day if at optimum temperature:

$$RLSEN(L) = RLV(L) \times RTSEN \times DTX \quad [13]$$

As a result of these equations, roots tend to grow and accumulate in moist soil layers and diminish in the saturated or drying soil layers (less than 25% available water). Typically, the simulated RLD of the top 5-cm layer is less than that in the 5- to 15-cm layer because of more frequent soil drying, despite both layers having the same soil hospitality factor.

Simulated rooting depth over time is compared in Fig. 3–2 to reported rooting depth for 'Wayne' soybean grown on a silt loam soil in 1979 at Castana, IA (Mason et al., 1980). The RTPROG is simulated reasonably well, but CROPGRO assigns a rooting depth (25 cm) at emergence, and the rate of depth increase should be slightly faster if the initial depth at emergence were to be reduced.

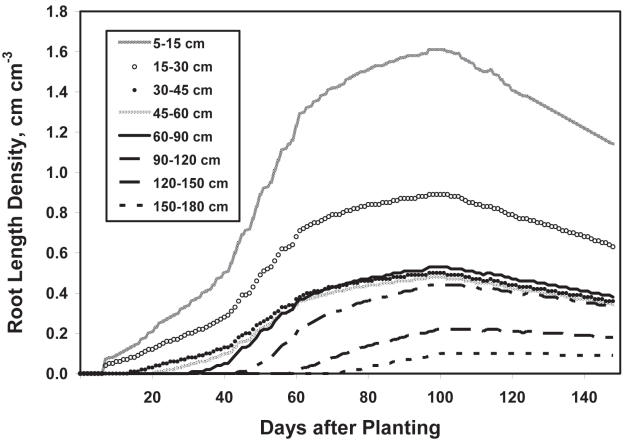

Fig. 3–3. Simulated RLD over time for successively deeper soil layers for Florunner peanut sown 1 Apr. 1981 at Gainesville, FL. Crop was irrigated but simulations indicated minor water deficit during 43 to 61 d, and again 114 to 120 d after sowing.

Similarly, the rate of simulated rooting depth progression for peanut was set by calibration to maximum depth of water extraction (from tensiometer measurements) and root observation over time for 'Florunner' peanut grown on a Lake fine sand (loamy, siliceous, hyperthermic *Grossarenic Paleudults*) in Gainesville, FL (Boote et al., 1983). The observed depth progression was 2.2 to 2.8 cm d^{-1}. In addition, the simulated rooting depth profile over time for crops such as peanut (Fig. 3–3) were calibrated to reproduce the observed RLD profile vs. depth measured at full canopy development (65–95 d) by Robertson et al. (1980). The SRGF(L) function for peanut for this Millhopper (or Lake) fine sand soil was 1.0, 0.55, 0.32, 0.38, 0.40, 0.30, and 0.20, respectively, for the 15, 30, 60, 90, 120, 150, and 180 depths. Figure 3–3 shows abundant rooting in topsoil to 30 cm, poor rooting in the tillage pan (30–60 cm), and relatively better rooting preference at deeper depths.

Root penetration and proliferation as they are affected by the static and dynamic characteristics of the soil layers (e.g., soil water content and temperature) in the DSSAT models, needs improvement, particularly to better account for soil impedance associated with different soil textures, bulk density, and soil water status. A number of the ideas for modeling root length growth proposed by Jones et al. (1991) are worthy of reinvestigating. Figure 3–4 illustrates simulated soybean RLD with a default exponential decline equation for SRGF(L) (equation given in Table 3–1) compared with the RLD based on modified SRGF function currently used that accounts for plow pan below 15 cm and creates a good root hospitality factor at depth to increase root proliferation in deeper layers in this Ida silt loam soil (fine-silty, mixed, calcareous, mesic *Typic Udorthents*) at Castana, IA. The observed RLD on Day 232 (maximum rooting at start of grain growth) is shown in Fig. 3–4, but is multiplied by a factor of 2.0 to approach the values of the

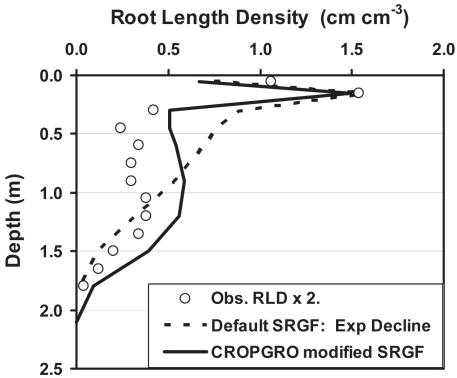

Fig. 3–4. Simulated RLD with the DSSAT default function (exponential decline with depth, equation given in Table 3–1) compared with the simulated RLD based on modified SRGF function that accounts for plow pan below 15 cm but gives good root proliferation in deeper layers in a Ida silt loam soil at Castana, IA, in 1979 (data from Mason et al., 1980).

Table 3–1. Soil Root Growth (preference) Function (SRGF) used to distribute roots to soil layers, and resulting simulated root length density (RLD) for two Iowa soils. DSSAT default uses an exponentially declining function: SRGF = 1 * EXP(−0.02 * LAYER_CENTER). Default is the same for the Nicollet clay loam soil or Ida silt loam soil. The modified SRGF for Nicollet clay loam resulted from fitting soil water extraction. The modified SRGF for Ida silt loam was fit to observed root distribution as well as soil water extraction.

	Nicollet clay loam			Ida silt loam		
Soil layer	SRGF-default	SRGF-modified	Sim RLD† Day 223	SRGF-modified	Sim RLD† Day 232	2 × Obs‡ RLD Day 232
(cm to bottom)	0–1.0	0–1.0	cm cm^3	0–1.0	cm cm^3	cm cm^3
5	1.000	1.00	0.51	1.000	0.68	1.06
15	1.000	1.00	1.41	1.000	1.49	1.54
30	0.638	0.83	1.53	0.257	0.51	0.42
45	0.472	0.80	1.40	0.257	0.51	0.24
60	0.350	0.77	1.25	0.263	0.54	0.34
90	0.223	0.66	1.01	0.300	0.59	0.30
120	0.122	0.60	0.86	0.300	0.56	0.38
150	0.067	0.51	0.53	0.300	0.40	0.27
180	0.037	0.50	0.27	0.300	0.09	0.08
202	0.020	0.50	0.02	0.300	0.00	–

† Simulated RLD using the modified SRGF.

‡ Observed RLD data from Mason et al. (1980).

CROPGRO simulations. Experimentally, RLD is difficult to measure and would typically be underestimated.

Evaluation of the Soil Water Balance and Evapotranspiration

Approach and Philosophy of Testing

As part of the process of evaluating and improving the model for use under water-limited conditions, the model must be tested for accurate prediction of soil

water extraction from successive layers by comparison with observed soil water contents during the crop life cycle. Inaccuracy in prediction of soil water balance can originate from poorly defined soil traits or faulty algorithms and coefficients for prediction of soil evaporation and plant transpiration. Inaccuracy in predictions of rooting front, assimilate allocation to roots, root length per unit mass, and water uptake per unit root length is also important.

The linkage between simulated soil water content, ET, and crop dry matter accumulation is sufficiently strong that problems in the simulated soil water balance or ET will show up as problems in predicted crop dry matter accumulation. Failure to accurately predict water deficit, can be attributed to several causes: (i) incorrect soil water-holding capacity (DUL–LL), (ii) incorrect simulated rooting profile or rooting depth front, (iii) incorrect simulated transpiration (related to PET option or wrong LAI or wrong extinction coefficient), and (iv) incorrect simulated soil evaporation. The soil water balance of the CROPGRO model has been tested several times against measured data on soil water content at various depths over time and against measured ET data for several different crops (Singh et al., 1994; Calmon et al., 1999; Nielsen et al., 2002; Naab et al., 2004; Sau et al., 2004). The PET options and extinction coefficients for partitioning of PET were tested by Sau et al. (2004). The water extraction front and rooting depth were tested in early model development by Boote (unpublished, 1995, 1996) using data on water extraction front (Boote et al., 1983) and root distribution (Mason et al., 1980; Robertson et al., 1980) as discussed previously.

Simulated versus Observed Soil Water Content, Evapotranspiration, and Dry Matter Growth of Faba Bean

A rigorous test of PET options was conducted with soil water content data measured with a neutron probe to a depth of 1.95 m for rainfed faba bean (*Vicia faba* L.) grown on a deep alluvial low-impedance soil in two different seasons at Cordoba, Spain (Sau et al., 2004). The soil was deep and uniform and rainfall was sufficiently low during the dominant spring growing seasons that the time-series for ET could be estimated from regular neutron probe measurements of soil water content to a depth of 1.95 m for the rainfed crop without concern for deep drainage. Crop dry matter growth was measured over time, and used as an independent verification of when crop transpiration was first reduced (e.g., reduced crop assimilation). Root length density was measured, confirming the simulated root distribution profile to drive root water uptake. Sau et al. (2004) tested several PET options in combination with variation in the KEP for LAI extinction of total solar radiation. Sau et al. (2004) used the CROPGRO–Faba bean model (Boote et al., 2002) to compare simulated vs. observed soil water content of respective soil lay-

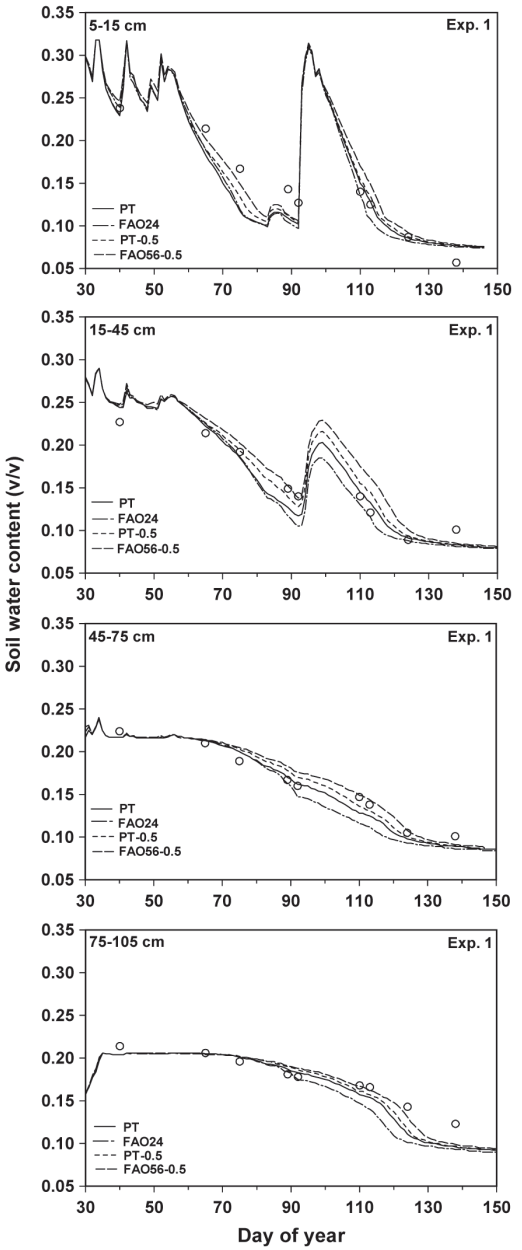

Fig. 3–5. Observed and simulated dynamics of soil water content of different soil layers during 1986–1987 season at Cordoba, Spain, simulated by CROPGRO-faba bean model using four PET options: (i) Priestley-Taylor (PT), (ii) FAO-24 Penman (FAO24), (iii) Priestley-Taylor with extinction coefficient of 0.5 (PT-0.5), and (iv) Penman-Montieth FAO-56 for reference crop with extinction coefficient of 0.5 (FAO56–0.5). Figure modified from Sau et al. (2004).

ers to a depth of 1.65 m and simulated vs. observed cumulative ET over time for the two different seasons as affected by several PET options. As shown in Fig. 3–5 and Fig. 3–6, the soil water balance was generally simulated adequately, except that the Priestley-Taylor and FAO-24 options overpredicted soil water extraction,

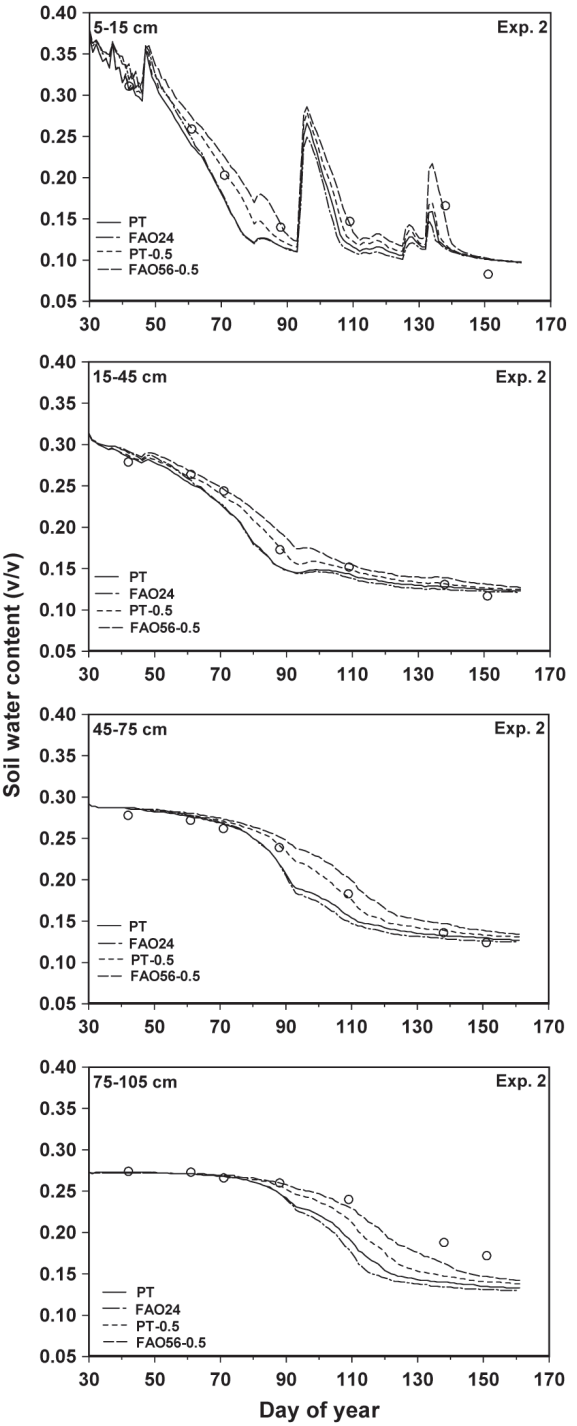

Fig. 3–6. Observed and simulated dynamics of soil water content of different soil layers during 1987–1988 season at Cordoba, Spain, simulated by CROPGRO-faba bean model using four PET options: (i) Priestley-Taylor (PT), (ii) FAO-24 Penman (FAO24), (iii) Priestley-Taylor with extinction coefficient of 0.5 (PT-0.5), and (iv) Penman-Montieth FAO-56 for reference crop with extinction coefficient of 0.5 (FAO56–0.5). Figure modified from Sau et al. (2004).

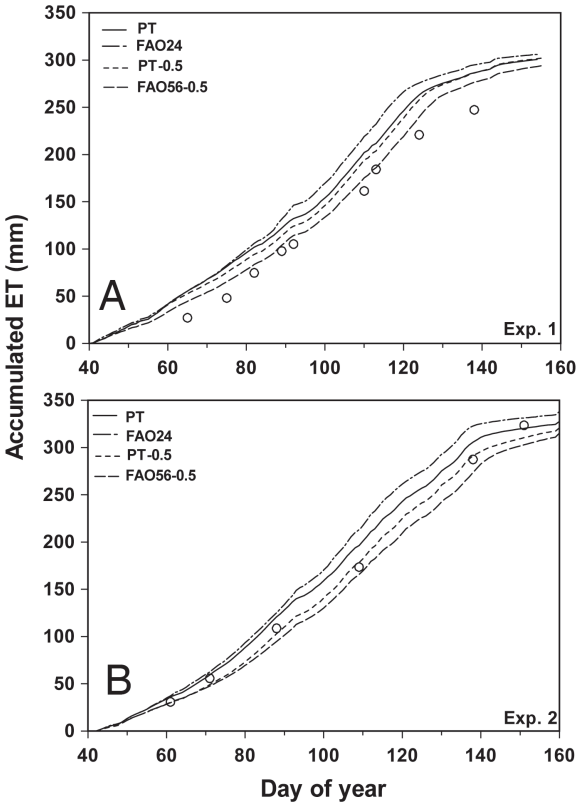

Fig. 3–7. Observed and predicted ET over time, as simulated with CROPGRO-faba bean model in: (A) 1986–1987, and (B) 1987–1988 seasons at Cordoba, Spain, using four PET options as described in Fig. 3–5 and Fig. 3–6. Figure modified from Sau et al. (2004).

especially early in the season when the old KEP value of 0.85 was used. Using a KEP value of 0.50 for the Priestley-Taylor option improved the predictions of soil water content, although the FAO-56 option with KEP of 0.50 most closely agreed with observations. Using the FAO-56 option gave the best predictions of the soil water balance (Fig. 3–5 and Fig. 3–6) and the time-series ET for both years (Fig. 3–7). Using a KEP of 0.50 for the extinction coefficient for the Priestley-Taylor (PT) option improved the prediction of seasonal ET during early season (Fig. 3–7) and improved the predicted soil water extraction during the early season for both years (Fig. 3–5 and Fig. 3–6) when the LAI was low and the extinction coefficient has its largest effect. Lastly, these effects on soil water balance and ET were also apparent in the "too-early" predicted reduction in dry matter accumulation for the Priestley-Taylor and FAO-24 PET options (Fig. 3–8). Based on these results, we recommended a lower KEP for all the DSSAT crop models, and recommended against using the FAO-24 Penman option. The good performance of the FAO-56 equation agrees with the conclusions of the 1998 FAO manual (Allen et al., 1998). As a result of this work by Sau et al. (2004), the DSSAT V4 models were modified;

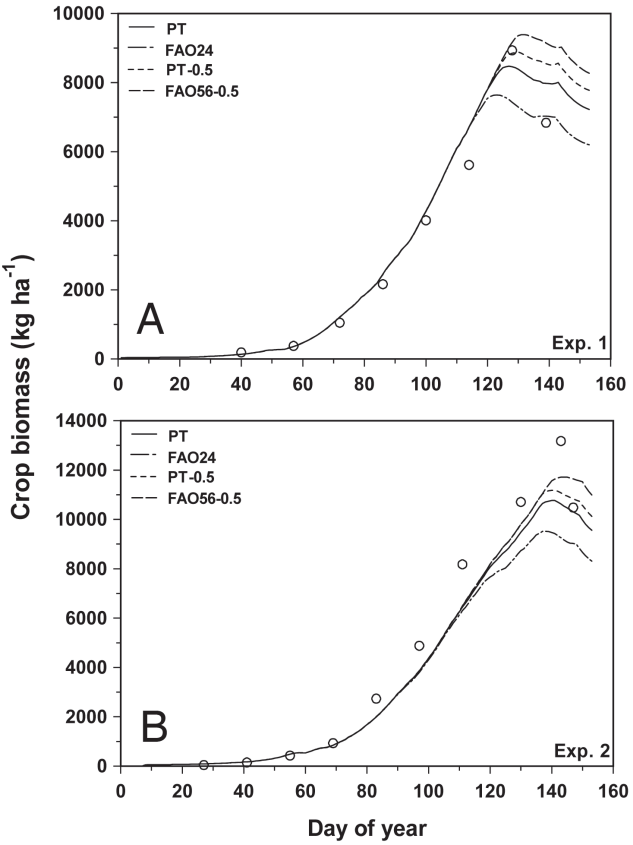

Fig. 3–8. Observed and predicted aboveground crop dry matter accumulation over time, as simulated with CROPGRO-faba bean model in: (A) 1986–1987, and (B) 1987–1988 seasons at Cordoba, Spain, using four PET options as described in Fig. 3–5 and Fig. 3–6. Figures modified from Sau et al. (2004).

the KEP was reduced from 0.85 to 0.70 for the CROPGRO model, and from 1.00 to 0.68 for the CERES-Maize crop model. (Note: Going all the way to KEP of 0.50 for all DSSAT models caused prediction of too little water-deficit, but other model parameters such as early rooting depth and root mass may have been incorrectly calibrated as offset to predict correct degree of water stress.) The Priestley-Taylor PET option was a good option if used with a lower KEP. Eitzinger et al. (2004) reported that CERES–Wheat (*Triticum aestivum* L.) and CERES-Barley (*Hordeum vulgare* L.; using Priestley-Taylor PET option with KEP of 1.0) and other wheat/barley models with the PT option, overestimated soil water extraction during the early season for three soils in Austria. Recent comparisons of simulated soil water contents and dry matter production of maize under rainfed conditions showed that CERES–Maize (*Zea mays* L.) overestimated soil water extraction and underestimated growth, although a lower KEP improved performance considerably (Lopez-Cedron et al., 2008). Nielsen et al. (2002) tested the CROPGRO–Soybean Version 3.5 model under water-deficit conditions with the PT option and a KEP of

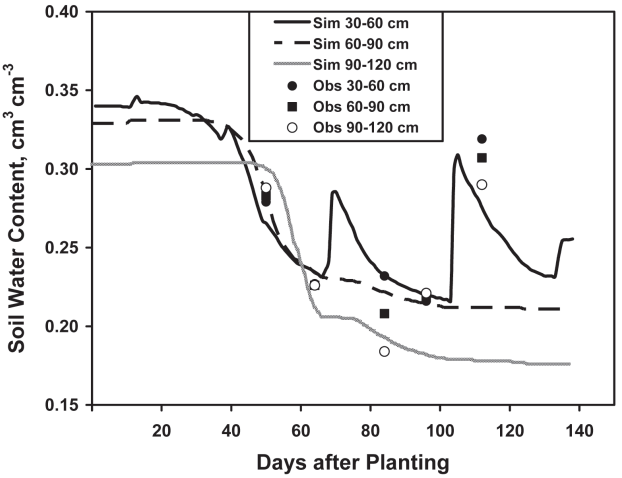

Fig. 3–9. Simulated and observed soil water content for 30- to 60-, 60- to 90-, and 90- to 120-cm layers of Nicollet clay loam soil, on which 'Williams 82' soybean was grown under rainfed conditions at Ames, IA, in 1988 (data courtesy of R. M. Shibles). A rainfall of 142 mm occurred on Day 103.

0.85. Although they reported a good overall performance, their results showed a similar tendency for an overprediction of ET during the first part of the growing season. Thus, multiple studies confirm the tendency of PT option to overpredict ET when used with older, high KEP values. However, the PT option is often the only option when windrun and dewpoint temperature are not available, and the PT option is acceptable if used with lower KEP.

Simulated versus Observed Soil Water Content, Evapotranspiration, and Dry Matter Growth of Soybean at Ames, Iowa, during the 1988 Drought

The American Soybean Association funded soybean model evaluation studies in 1988 and 1990 on 'Williams 82' soybean grown under rainfed conditions at Ames, Iowa (unpublished data, courtesy of R.M. Shibles, 1990). The 1988 season is well known as the 1988 Midwestern drought, and allowed us to contrast growth of the 1988 rainfed crop to growth of the same cultivar on the same soil in the cool and rainy season of 1990. During the 1988 experiment, soil water content was measured with a neutron probe.

These 1988 Ames, IA, data were valuable for illustrating the importance of the potential root distribution function, for highlighting deficiencies in the infiltration function (curve number approach), and testing crop growth and ET response. Figure 3–9 shows the simulated soil water contents of several soil layers over time and Fig. 3–10 shows total plant extractable soil water to a depth of 202 cm. These comparisons are not a true validation, as modifications to the rooting profile shown in Table 3–1 were necessary to create greater root proliferation at depth for extracting the soil water from the deeper soil layers (90–120-cm soil depth, for example) as well as delaying the onset of water deficit observed in crop

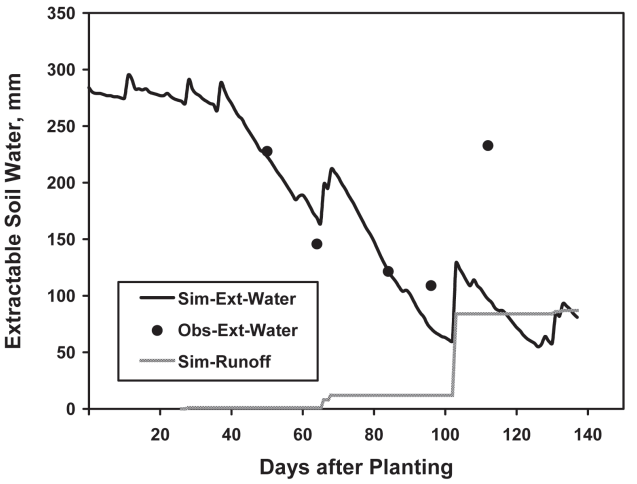

Fig. 3–10. Simulated and observed total plant extractable soil water to 202-cm depth and simulated runoff for Williams 82 soybean grown on Nicollet clay loam soil under rainfed conditions at Ames, IA, in 1988 (data courtesy of R. M. Shibles, 1990). A rainfall of 142 mm occurred on Day 103.

growth. A greater fraction of RLD had to be placed at deeper soil layers than was generated by the default option by the DSSAT V3.5 soil creation program (Table 3–1). In addition, the soil water holding traits of the Nicollet clay loam soil were slightly modified. These simulations highlight the poor behavior when using default assumptions such as an exponentially declining rooting probability function, which is the default for DSSAT soils creation program if users have no information. Another interesting dynamic occurred about 103 d after planting, when a large 142-mm rainfall apparently infiltrated to a depth of 120 cm, but the simulated soil water balance did not pick this up. The simulated runoff from this event was 72 mm (Fig. 3–10), which was obviously not correct. What probably happened in this field was that water infiltrated down cracks in this cracking clay loam soil and the water was not lost to runoff. This highlights a problem in the Soil Conservation Service curve number approach for soil water infiltration. In this particular study, the rainfall came relatively late and the excessive simulated amount of runoff, if infiltrated, would not have made much difference in growth and yield. But yield response would have been much more if the rainfall event had been a month earlier.

The simulated and observed soybean crop growth was initially more rapid in the warm, droughty season of 1988 compared with the cool, rainy season of 1990 (Fig. 3–11), and the model nicely picked up this difference. But water deficit after 85 d in 1988 eventually limited dry matter growth of the total crop and pods, causing lower biomass and yield at harvest. The modified deeper rooting profile described above was necessary to mimic the correct (lesser) reduction in crop and pod mass accumulation as well as the correct (deeper) soil water extraction. Even

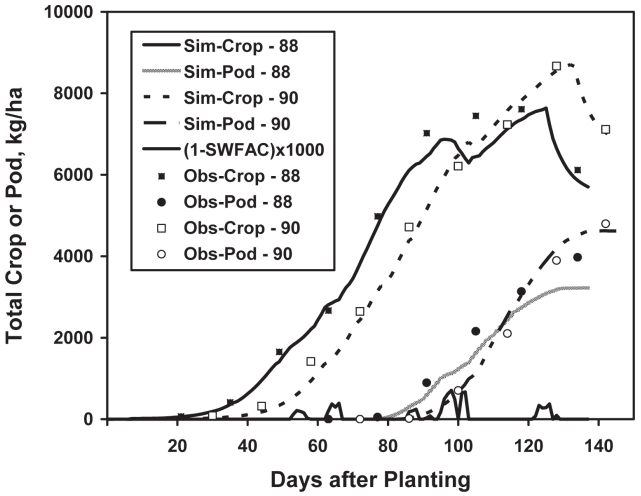

Fig. 3–11. Simulated and observed total crop dry matter and pod dry matter accumulation over time for Williams 82 soybean grown on Nicollet clay loam soil under rainfed conditions at Ames, IA, in 1988 and 1990 (data courtesy of R. M. Shibles, 1990). The 1988 season was warm and droughty, while the 1990 season was cool and rainy.

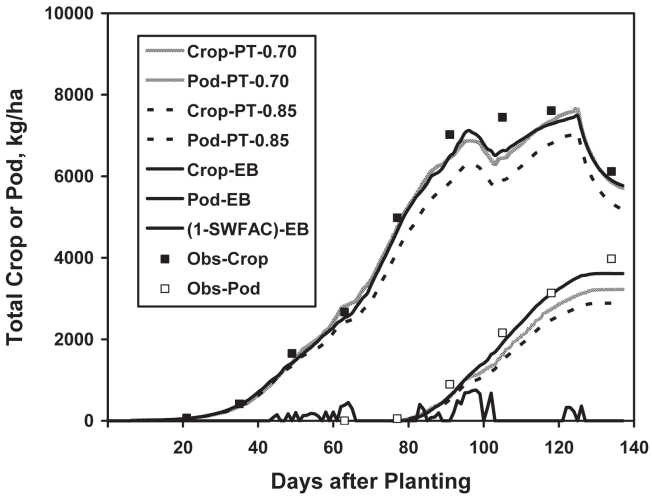

Fig. 3–12. Total crop and pod dry matter accumulation as simulated by the hourly energy balance (EB) option or the Priestley-Taylor PET option with extinction coefficient for transpiration (KEP) of 0.70 (current, PT-0.70) or 0.85 (old-V3.5, PT-0.85). Observed data for Williams 82 soybean grown on Nicollet clay loam soil under rainfed conditions in 1988 at Ames, IA, (data courtesy of R.M. Shibles, 1990).

so, there was too much delay in pod growth, showing the need for accelerating reproductive growth under water deficit as will be discussed later.

Good neutron probe measurements for the 1988 Ames, IA, season as well as the lack of significant rainfall after planting that minimized drainage allowed us to compute the observed ET for comparison to simulated ET. The availability of weather data with windspeed and dewpoint temperature allowed us to test the hourly energy balance (EB) option for predicting ET, and to contrast that to predictions with the Priestley-Taylor PET option using 0.70 or 0.85 as the KEP for partitioning of PET to EP_O. Figure 3–12 illustrates how changing the KEP from 0.85 to 0.70 improved the predictions of crop and pod dry matter accumulation

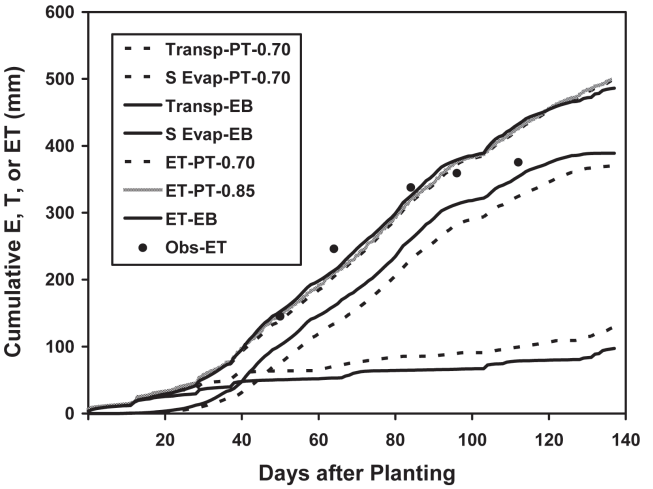

Fig. 3–13. Prediction of ET, soil evaporation (S Evap-PT-0.70), and EP (Transp-PT-0.70) for the Williams 82 soybean study at Ames, IA, in 1988, with the hourly energy balance option (EB) compared with the Priestley-Taylor option with KEP of 0.70 or 0.85.

in the 1988 Ames, IA, drought. This confirms findings of Sau et al. (2004) that the KEP needs to be lower than that for extinction of photosynthetically active radiation. The hourly energy balance option of the model (simulated with V3.5) is also shown in Fig. 3–12 and was shown to give good biomass predictions comparable with the use of the PT option with KEP of 0.70. This comparison is important because the hourly energy balance uses an entirely different method for simulating soil evaporation and transpiration; it also has its own built-in partitioning to E and T and does not use KEP at all. This also confirms the need to reduce KEP from 0.85 to 0.70. With the PT option, the effect of KEP (0.70 vs. 0.85) on total ET was minor (Fig. 3–13) because the crop could only extract what water was available, but the improved dry matter accumulation resulted because of conservation of soil water early in the season, and because more of the ET was used for T rather than E. The hourly energy balance model (EB) predicted nearly the same seasonal ET, but importantly, the EB option allocated more water to transpiration and less to soil evaporation, thus also effectively conserving water for transpiration, photosynthesis, and dry matter accumulation (like a lower KEP had done). We have suspected that the soil evaporation of the DSSAT models may be high; therefore we tend to believe this trend of the hourly energy balance option. These results highlight the need to look further at methods for predicting soil evaporation, especially to consider effects of narrow row spacing and no-till residue coverage.

The somewhat higher pod dry matter growth for the hourly energy balance option is related to an entirely different matter (the simulated foliage temperature in late season in Iowa was predicted to be warmer than air temperature which increased seed growth over the standard model which uses air temperature to drive seed growth). The energy balance option uses foliage temperature to drive

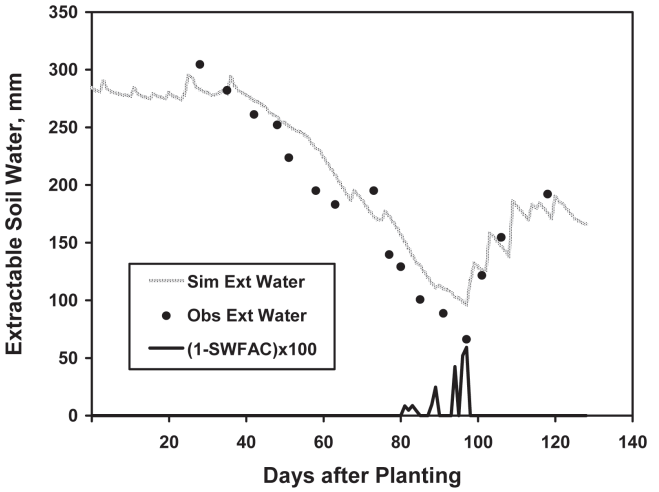

Fig. 3–14. Simulated and observed extractable soil water over time for Wayne soybean grown in Ida silt loam soil at Castana, IA, in 1979 (data from Mason et al., 1980). The simulated SWFAC is shown as (1-SWFAC) × 100.

all aerial growth processes. Emergence was a day later because of cooler soil temperature, but the crop life cycle was shorter by 1 d because foliage temperatures tended to be above air temperature, at least early and late in the season.

Simulated versus Observed Rooting Pattern, Soil Water Balance, and Dry Matter Growth of Soybean at Castana, Iowa

An excellent data set on soybean growth, soil water extraction, and RLD was available for the Wayne soybean cultivar grown under rainfed conditions in 1979 at Castana, IA (Mason et al., 1980). Wayne is a parent line of Williams 82 and thus has similar growth and life cycle. The soil for this study was a loess-derived silt loam soil that was uniform to 4 m or more, so there was no question about good soil hospitality to root growth, except for a plow pan below 15-cm depth. This was evident in the root growth pattern observed by Mason et al. (1980). Table 3–1 shows the input values for the SRGF function modified for the Ida silt loam soil to mimic the observed RLD profile as well as the soil water contents and extraction with depth. In setting the SRGF function, it is important to recognize that the model does not grow roots into a soil layer until the rooting front progresses into that zone, and that by itself will give a somewhat declining RLD with depth, even if the hospitality factor is 1.0 all the way to the bottom of the profile. For this silt loam, we set a high value of 1.0 for the topsoil which had higher organic matter, followed by a low value for the restrictive plow pan (15–45 cm), followed by a higher SRGF the rest of the way down. This SRGF and the Priestley-Taylor ET option with KEP of 0.70 (V4.0 default) were used to simulate the plant extractable soil water over time (Fig. 3–14) and the dry matter growth of total crop and pod (Fig. 3–15). SWFAC increased as the plant extractable water in the profile

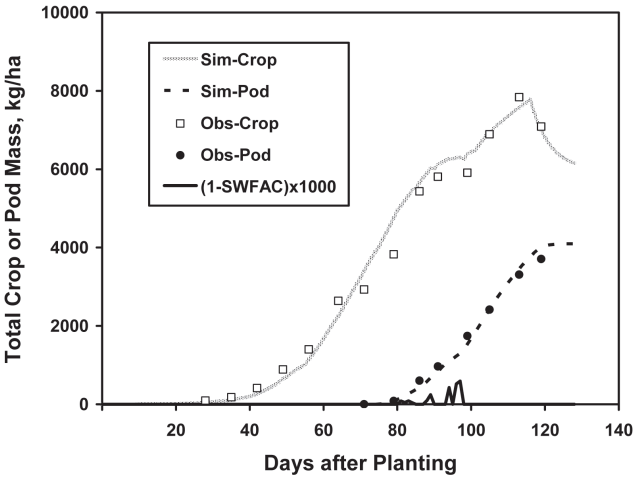

Fig. 3–15. Simulated and observed total crop and pod dry matter accumulation over time for Wayne soybean grown in Ida silt loam soil at Castana, IA, in 1979 (data from Mason et al., 1980). The simulated SWFAC is shown as (1-SWFAC) × 1000.

approached 100 mm about 80 d after sowing. After calibrating SRGF using the observed root data, rather than using default SRGF values from the DSSAT soil creation program, the simulated water contents (individual layers not shown in Fig. 3–14) were predicted well in most soil layers except for the top 5-cm zone where the model predicted too much water loss (associated with soil evaporation routine), and for deeper depths below 150 cm, where extraction was too late because the simulated root depth progression (with default model parameters) was slower than observed. From these results, we conclude that the tipping bucket soil water balance per se works well, but improvements are needed in the root growth routine, e.g., how fast to grow rooting depth/front and where to place the roots.

Simulated versus Observed Soil Water Balance of Soybean on a Sandy Soil at Gainesville, Florida

Our group at Gainesville, FL, has grown 'Bragg' and 'Cobb' soybean under rainfed and irrigated conditions on a Millhopper fine sand (loamy, siliceous, hyperthermic *Groassarenic Paleudults*) soil in various years. While we measured dry matter growth in all years, we only measured soil water in some years. Figure 3–16 illustrates the simulated plant extractable soil water (to 1.95-m depth) over time for 'Bragg' grown under rainfed conditions in 1978 during which a major drought and water stress occurred, sufficient to reduce yield to about one-third of the irrigated treatment. The results shown in Fig. 3–16 cannot be considered an independent evaluation, as various parameters of crop C balance and soil water balance were modified as part of our process of SOYGRO and CROPGRO model improvements over the years. Rainfall was so frequent during 40 to 60 d after sowing that water actually was simulated to temporarily perch in the 1.50- to

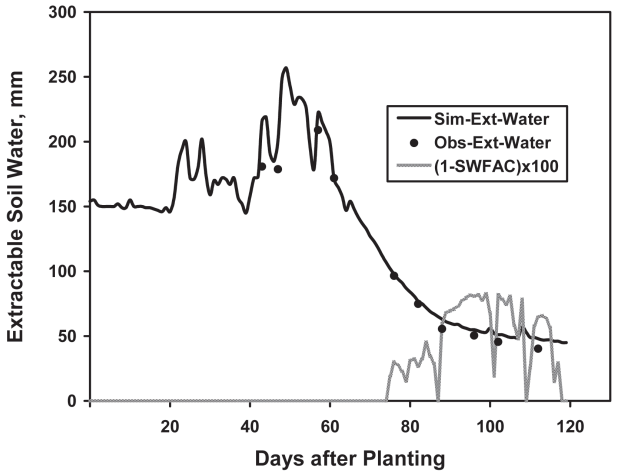

Fig. 3–16. Simulated and observed plant extractable soil water over time for Bragg soybean grown under rainfed conditions at Gainesville, FL, in 1978. Also shown is (1-SWFAC) × 100, to illustrate severe water stress during last half of the season.

2.10-m zone of this soil and may have contributed to crop survival and subsequent grain production during a 61-d period in which 33 mm of rain fell.

Simulated versus Observed Soil Water Balance of Peanut in Ghana

Data on simulated vs. observed peanut growth and soil water in Ghana were reported by Naab et al. (2004). Using field-estimated values for DUL and LL, the model simulated the soil water contents quite well for soil layers down to 0.90 m (Fig. 3–17). Similarly, Singh et al. (1994) found that the tipping bucket soil water balance and Priestley-Taylor option predicted soil water extraction well for many peanut data sets in India. We found no major problems with the simulated soil water contents compared with soil water contents measured in about 21 on-farm and on-station experiments of peanut (Boote et al., 1989; Gilbert et al., 2002). The larger questions were typically estimating DUL and LL, as well as how far roots progressed with depth, which affected soil water later in the season and affected the degree of stress on dry matter accumulation. In addition, there were some obvious situations where the simulated dry matter growth was too high, but these were typically associated with rootknot nematode or disease during the last half of the season on peanut in Ghana, India, and Florida.

Simulating Effects of Water Stress on Growth and Development Processes

This section gives examples and discusses how two water stress signals, SWFAC and TURFAC, affect photosynthesis, expansive growth, partitioning, and phenological development. Recall that SWFAC and TURFAC are both computed from the ratio of potential root water uptake to EP_O based on the daily weather.

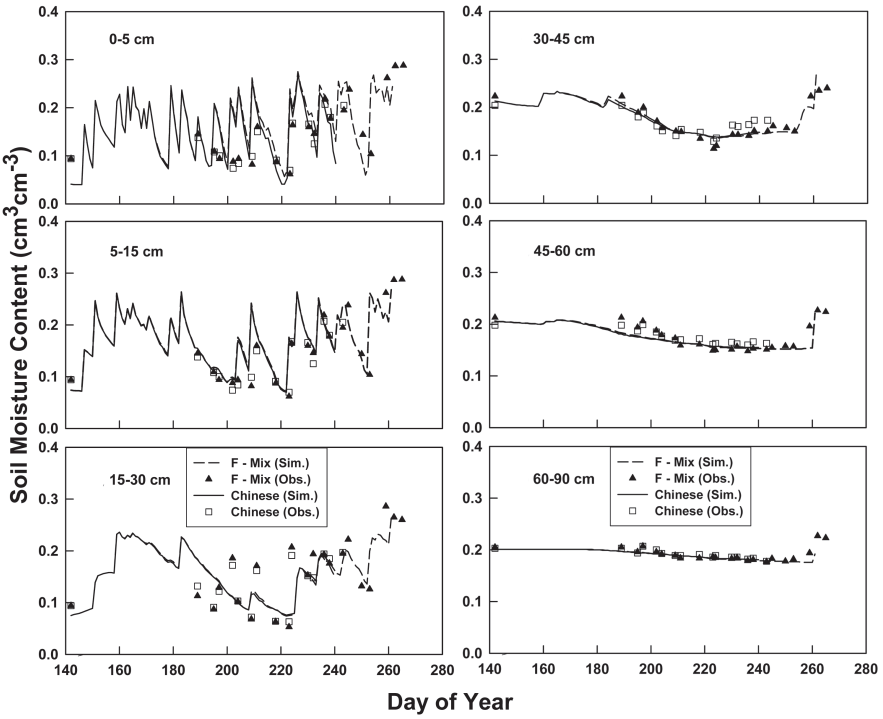

Fig. 3–17. Soil water balance simulations with the CROPGRO-Peanut model for six soil layers at Tamale, Ghana, using field-estimated values for DUL and LL. Figures used with permission from Naab et al. (2004).

Sensitivity of Photosynthesis to Water Deficit

In CROPGRO, dry matter accumulation depends directly on crop canopy photosynthesis. When the SWFAC signal falls below 1.0, then daily photosynthesis and transpiration are reduced in a one-to-one manner. This assumption is a mimic of stomatal action, allowing CO_2 to be fixed in proportion to transpiration. CROPGRO with the daily PET options has no vapor pressure deficit effect on photosynthesis or on stomatal function. CROPGRO's hourly energy balance option does have explicit stomatal conductance responsive to energy balance (and it includes vapor pressure effects on transpiration, EB, and foliage temperature). Effects of soil water deficit on photosynthesis are evident in reduced rates of accumulation of dry matter, as highlighted in several figures in this chapter; but the correctness of prediction depends on accuracy of soil water holding capacity, infiltration, rooting depth progression, rooting profile shape, PET options, extinction partitioning coefficients, as well as the crop model's rooting response to drought (partitioning shift and accelerated rooting depth). Simulated dry matter accumulation in rainfed versus irrigated Bragg soybean in 1978 (Fig. 3–18) is a

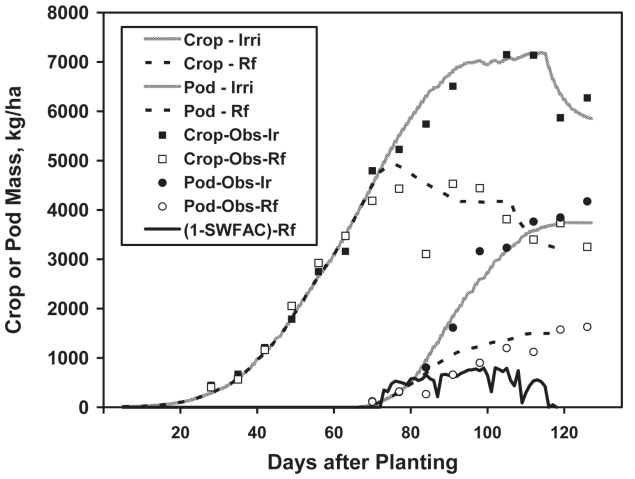

Fig. 3–18. Simulated total crop and pod dry matter accumulation of rainfed and irrigated Bragg soybean in 1978 at Gainesville, FL. Also shown is (1-SWFAC) × 1000, to illustrate severe water stress during the last half of the season (data from Wilkerson et al., 1983).

good example of a reduction in dry matter accumulation in response to soil water deficit. This figure also shows the magnitude of water stress over time.

Crop Developmental Rate under Water Deficit

Progression of the crop through its various successive life cycle phases is modeled in CROPGRO as a function of physiological day accumulation, which depends on both temperature and daylength sensitivity. CROPGRO's cultivar files specify the critical daylength sensitivities and phase durations. The species file contains the cardinal base and optimum temperatures for the species and coefficients for each given life cycle phase to designate slower (delayed) or accelerated development under water deficit. For full details on the phenology submodules of CROPGRO see the 2004 DSSAT V4 crop model documentation (Jones et al., 2004, p. 1–21). Time to emergence, for example, depends on mean soil temperature and soil water availability in the top 10 cm of soil. Subsequent life cycle phases depend on hourly air temperature computed from maximum and minimum air temperature using a sine-exponential delay function (Parton and Logan, 1981; Kimball and Bellamy, 1986) and a modifying effect of soil water [FSW(J)], computed from SWFAC and a phase-sensitive factor WSENP(J) as shown in Eq. [14]:

$$FSW(J) = 1.0 + (1.0 - SWFAC) \times WSENP(J) \quad [14]$$

In CROPGRO-Soybean, SWFAC is allowed to cause mild delays in reproductive progression to beginning flower/pod/seed (−0.40) and stronger delays of end of leaf expansion (−0.60 to −0.90) using growth-phase-specific modifiers. By contrast, SWFAC strongly accelerates progression from beginning seed to maturity (+0.70). There are several papers showing that water deficit accelerates physiological maturity (phase length after beginning seed) in soybean (Desclaux and

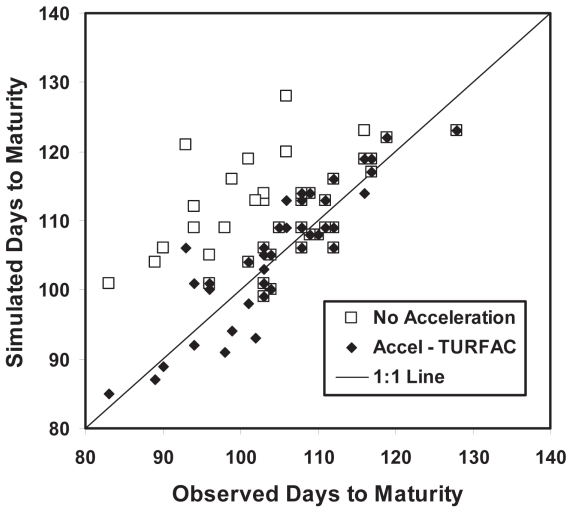

Fig. 3–19. Predicted physiological maturity in soybean as simulated with the CROPGRO-Soybean model with acceleration (as a function of TURFAC) or no acceleration, using 26 irrigated treatments and 16 rainfed treatments of two cultivars over five seasons at Lugo, Spain. Figure used with permission from Ruíz-Nogueira et al. (2001).

Roumet, 1996; Ruíz-Nogueira et al., 2001), dry bean- *Phasolus vulgaris* L. (Boote, unpublished data, 1986), and faba bean (Sau and Minguez, 2000). The CROPGRO-Soybean model predicted accelerated maturity well (Fig. 3–19) for soybean grown under rainfed vs. irrigated conditions in Spain (Ruíz-Nogueira et al., 2001) when using TURFAC (in a test version) for acceleration effect. TURFAC was found to be an improvement over using SWFAC for acceleration, because SWFAC was late in acting. It appears that species differ in whether there is delay or acceleration of these reproductive phases, as we have observed strong acceleration of onset of reproductive growth (pod number, pod and seed mass, and pod harvest index) in chickpea (*Cicer arietinum* L.) and faba bean (Sau and Minguez, 2000) and moderate acceleration in dry bean and soybean, but actual delay in peanut.

Rate of Leaf Appearance under Low Plant Turgor

The rate of node/leaf appearance on the main axis (V-stage) is a type of vegetative phenology. Rate of leaf appearance uses Eq. [15] (given in integration form) that incorporates TURFAC effects to slow node appearance rate below that driven by the physiological day accumulation (DTX) and the genetic potential node appearance rate (TRIFOL). TRIFOL is the number of leaves that appear per day if at optimum temperature all day long. As the actual daily fraction partitioning of assimilate to pod and seed (XPOD) increases, the factor (1.0 − XPOD) will slow leaf appearance rate as a function of assimilate shortage.

$$\text{VSTAGE} = \text{VSTAGE} + \text{DTX} \times \text{TRIFOL} \times \text{TURFAC} \times (1.0 - \text{XPOD}) \quad [15]$$

Reduction of Expansive Processes under Low Plant Turgor

The vegetative expansion processes of leaf area expansion, main stem node appearance rate, and canopy height increase are proportional to TURFAC. This effect is beyond the primary water deficit effect to reduce photosynthesis. A TURFAC less than 1.0 reduces the rate of leaf appearance (V-stage), specific leaf area of new leaves, height increase (internode elongation), and width increase. It also shifts fraction plant allocation toward root, and shifts the shoot C allocation from stem toward leaf. Together, these actions reduce canopy size and LAI under plant water stress. In fact, these expansive processes and the shift in partitioning to roots begin at a plant water status at which photosynthesis and dry matter accumulation are not yet reduced (Fig. 3–1 shows that TURFAC is 0.67 when SWFAC is still 1.0). This feature mimics reports in literature suggesting that vegetative expansion processes are limited sooner than photosynthesis under water limitation.

Enhanced Partitioning to Roots under Water Deficit

On any day when there is water stress or N stress, partitioning of assimilate to roots, Xr, is enhanced as a function of TURFAC or NSTRES using the following equation:

$$Xr = Xro + ATOP \times [1 - MIN(TURFAC, NSTRES)] \times (1 - Xro) \quad [16]$$

where NSTRES is the ratio of today's N supply to N demand, Xro = normal partitioning to roots, and ATOP is the maximum change in partitioning under severe water deficit, i.e., when TURFAC is zero. ATOP is typically 1.00, so if 80% of new growth is normally partitioned to tops and 20% to roots, then as stress increases (as TURFAC approaches 0.0), all the new growth is partitioned to roots. This approach has worked nicely to mimic the observed increase in root/shoot ratio under water deficit or N stress. It is also an adaptive response, rather than a constitutive response, that actually improves crop yield response under water deficit by about 4% for an ATOP of 1.00 without affecting yield potential under good water status (Boote and Jones, 1986; Boote et al., 2003). Figure 3–20 illustrates how this TURFAC-dependent function caused nearly twice the simulated total root mass in the continuously stressful drought in 1988 at Ames, IA, compared with the rainy 1990 season, despite somewhat less total biomass production.

Shift in Partitioning to Leaf versus Stem after Water Deficit

With early model versions, we experienced a problem of too much simulated stem mass and too little simulated leaf mass following relief of water deficit during the vegetative phase. We suspect the problem is related to the need to link reduced dry matter partitioning to stems concurrently with already predicted shortening of internodes during water stress. Other causes could be reduced leaf abscission

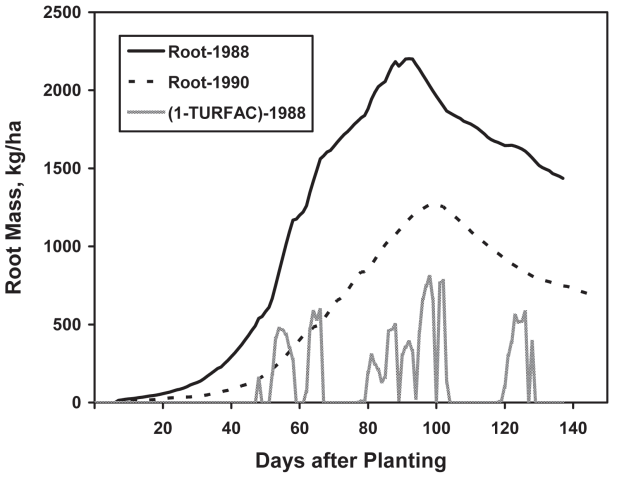

Fig. 3–20. Simulated root mass of Williams 82 soybean grown in 1988 drought year compared with the 1990 rainy season at Ames, IA. Simulated TURFAC is shown as (1-TURFAC) × 1000.

after the water deficit is relieved, as well as the higher light regime of the smaller water-stressed crop that would allow more leaves to be retained after the water stress period. To mimic this behavior, we created a rolling 20-d memory of the turgor factor (CUMTUR) as coded in Eq. [17–20], which is used to shift partitioning (among leaf and stem) toward leaf, but with a delay effect that extends after the stress has ended. FRRT is the same as Xr, fraction allocation of daily plant dry matter growth going to root. FRLF and FRSTM are fraction of daily shoot dry matter growth going to leaf and stem, respectively.

$$\text{CUMTUR} = 0.95 \times \text{CUMTUR} + 0.05 \times \text{TURFAC} \quad [17]$$

$$\text{FRLF} = [1.0 + 0.6 \times (1.0 - \text{CUMTUR})] \times (1.0 - \text{FRRT}) \times \text{FRLF}/(\text{FRLF} + \text{FRSTM}) \quad [18]$$

$$\text{FRLF} = \text{MIN}[\text{FRLF}, 0.90 \times (1.0 - \text{FRRT})] \quad [19]$$

$$\text{FRSTM} = 1.0 - \text{FRRT} - \text{FRLF} \quad [20]$$

The value "0.6" is an arbitrary scalar that was optimized for soybean, although the value could be species-dependent. In future versions of the model this constant will be moved to the species file to allow for species-dependent responses. This constant should be in the species file, and it should be replaced with a more mechanistic handling of this process (such as shortened internodes means less partitioning to stem mass).

Enhanced Leaf and Petiole Senescence and Nitrogen Mobilization under Water Deficit

Leaf senescence is accelerated as a function of SWFAC (Eq. [21] and Eq. [22]). SENDAY is the maximum fraction of existing leaf mass (WTLF) that can be senesced on a given day as a function of severe water stress 4 d earlier ($n - 4$). SENDAY

is a species coefficient defined under the maximum water deficit when SWFAC equals zero. There is a 4-d lag in leaf abscission, created to give time for the leaf to yellow and fall off. The species file defines a maximum fraction of leaf, e.g., SENMAX = 0.60, that can be abscised from the plant at a given V-stage called XSENMX, despite the most severe water stress. Equation [22] is a "look-up" function that is passed the current VSTAGE and returns that maximum fraction SENMAX. The amount of leaf mass actually lost is restricted, so as to retain a given minimum fraction of leaf mass left (PORLFT) despite the outcome of Eq. [21]. These processes need to be made more mechanistic.

$$WSLOSS = SENDAY \times (1.0 - SWFAC_{n-4}) \times WTLF \quad [21]$$

$$PORLFT = 1.0 - TABEX(SENMAX, XSENMX, VSTAGE, 4) \quad [22]$$

Water-stress induces leaf abscission that is in addition to natural leaf senescence that occurs as a function of thermal time, N mobilization (to seed), and low light-induced senescence. Leaves that abscise due to water deficit also lose N at their current leaf N (protein) concentrations. Leaves that abscise from aging, N mobilization factors, and low-light effects, abscise at a minimum leaf N (protein) concentration (PROLFF). The N mobilization is slow during vegetative growth, but is faster during reproductive growth, and the N mobilization rate from vegetative tissue can be accelerated up to 50% in response to water deficit during seed growth.

Petiole abscission also occurs in the CROPGRO model, and is coupled to the rate of leaf mass loss, by a ratio called PORPT (0.58 for soybean), which means that 0.58 g of stem mass (petiole) is lost per gram leaf mass abscised. This is for all causes of leaf abscission. Thus, to the extent that leaf (mass) abscission is accelerated by water stress, the abscission of stem (petiole) mass is accelerated.

Sensitivity of Nodule Growth and Nitrogen Fixation to Water Deficit

Nodule growth rate (RGR) and specific nitrogenase activity (SNA) in CROPGRO are sensitive to plant water status as shown in Fig. 3–1. In an earlier version (CROPGRO V3.1), nodules were sensitive to the fraction available soil water in the nodule zone, a prevalent hypothesis a few years ago. This approach did not work well because the nodule zone (upper 30 cm) is very prone to drying even when there is adequate water below 30 cm to meet plant needs for transpiration. Beginning with CROPGRO V3.5 released in 1998, nodule growth and nitrogenase activity were modeled to be sensitive only to plant water status, basically the minimum of today's plant water stress or an 8-d running memory of plant water stress. The reason for the 8-d running memory is to allow a damage effect of past plant water deficit. Having nodules sensitive to plant water status is consistent

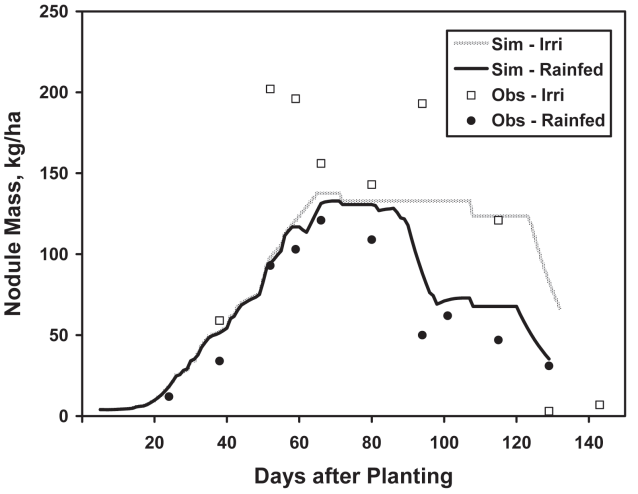

Fig. 3–21. Simulated and observed nodule mass over time for irrigated and rainfed Bragg soybean grown on a Kendrick fine sand (loamy, siliceous, hyperthermic *Grossarenic Paleudults*) at Gainesville, FL, in 1984. Observed data from DeVries et al. (1989b).

with data of Sprent (1972) who found that nodules in dry soil gained water from roots in moist soil. In addition, Albrecht et al. (1984) reported that SNA and nodule relative water content did not fully recover until the plant water status was fully recovered by irrigating deeply, despite good water status in the nodule zone.

CROPGRO allows crop species to have differential sensitivity of nodule RGR and SNA to plant water status. For soybean (Fig. 3–1), the sensitivity of nodules to water deficit is intermediate to the sensitivities of photosynthesis (using SWFAC) and vegetative growth (using TURFAC). Nodule growth and N fixation are sensitive to excess soil water (flooding) through anaerobic stress computed from the portion of pore space that is filled with water. When the pore space becomes completely water filled, both nodule growth and N fixation are restricted, and nodule senescence is enhanced. The flood sensitivity aspects of the model have not been tested sufficiently to set the minimum pore space that must remain air filled in the nodule zone to prevent anaerobic stress. Nodule death rate was set to a given daily fraction under stress, and this fraction is modified by the maximum of flooding (anaerobic) stress, water stress, or C shortage stress effects. Nodule death rate under water deficit conditions was calibrated to the nodule mass of the 1984-rainfed 'Bragg' experiment of DeVries et al. (1989b) as shown in Fig. 3–21, and we compared simulated N-fixation rate with N fixation data observed by DeVries et al. (1989a). Figure 3–22 shows simulated and observed SNA and simulated water stress over time for an irrigated treatment vs. a 19-d water deficit treatment during seed filling for Bragg soybean grown on a fine sand at Gainesville, FL, in 1980 (observed data from Albrecht et al., 1984). In that study, N fixation was

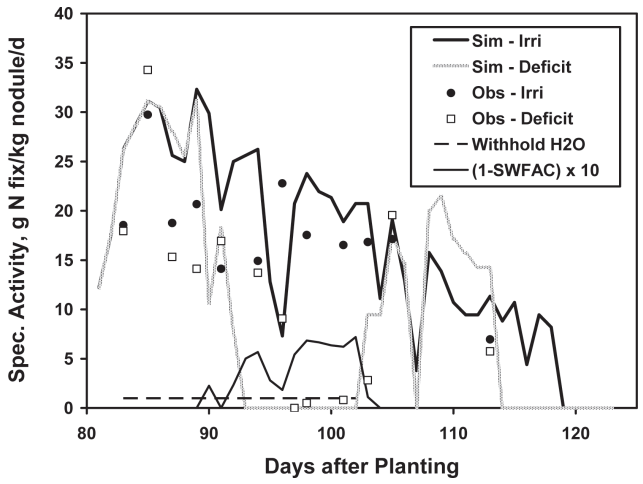

Fig. 3–22. Simulated and observed specific nitrogenase activity and the SWFAC signal over time for irrigated treatment vs. 19-d water deficit treatment during seed filling for Bragg soybean grown on a Millhopper fine sand at Gainesville, FL, in 1980. Observed data from Albrecht et al. (1984).

affected later by water deficit than was canopy assimilation, and N fixation recovered within 3 d after relieving water deficit.

Altered Nitrogen Uptake under Water Deficit

Potential N uptake per unit root length is a Michaelis-Menten function of the concentration of nitrate and ammonium in each layer, the RLD in each layer, and the soil water availability of that layer. The effect of the soil water availability factor on N uptake is quite sensitive, because N uptake has its optimum at DUL and is reduced as actual soil water is higher or lower than that DUL value. This sensitivity to soil water status has not been tested adequately, because CROPGRO has been used mainly for grain legumes and N fixation compensates for inadequate soil N availability. However, simulations of cotton (*Gossypium hirsutum* L.), tomato (*Solanum lycopersicum* L.), and forages with CROPGRO will require better evaluation of this function. Actual N uptake is the minimum of potential root N uptake and crop N demand. The model computes crop N demand from today's new growth times a target N concentration, plus a deficiency N demand. If computed crop N demand is less than potential root N uptake, the actual N uptake from each layer is proportionately scaled back from potential N uptake per layer. Since C assimilation is reduced under water deficit, the growth demand for N would also be less under water deficit.

Effects of Water Deficit on Pod Addition and Seed Growth

There is a minor direct reduction in the rate of potential flower/pod number added each day that occurs when SWFAC is less than 0.50, but this effect is small. More importantly, there is no direct water deficit effect on number of pods or seeds that

the crop can carry or on the single seed growth rate in CROPGRO, because effects of water deficit are already imposed on the photosynthetic rate that is the driver of pod addition rate, number of seeds carried at full seed load, and seed growth rate. Recent literature (Fisher, 2000) suggests that grain growth is less sensitive to low plant water potential than is the vegetative plant because the xylem hydraulic connection from the embryo or endosperm is blocked in the pedicel of cereal grain or seed coats of legumes, thus minimizing water return flow in xylem and improving seed water status. In addition, seeds receive a continuous supply of water with the phloem water flow to the seed. Thus, the appropriate mode for water stress effects on single seed growth rate is via the amount of photoassimilate available to drive phloem flow and seed growth.

Second-Order Effects of Water Deficit

There are many interactions that arise out of water deficit effects on multiple singular processes. For example, the water deficit-induced shift of assimilate to roots, reduced leaf expansion, and reduced height will cause smaller LAI and canopy size. This interaction we tend to understand. A more complex second-order reaction would be that the enhanced early root growth may cause greater tolerance to future water deficit, or that the reduced leaf area expansion results in thicker leaves that enhance subsequent photosynthesis per unit leaf area or reduce future leaf senescence due to low light effect under high LAI. Water stress acceleration of maturity of the crop is also an understandable feature, but it reduces the amount of time for grain fill (shorter phase), and grains will be smaller for that reason as well as from less assimilate per day.

Illustration of Modeled Crop Growth Responses to Water Deficit

Growth analysis data of soybean were collected on 'Bragg' (MG 7) in 1978 and 1984, and 'Cobb' (MG 8) in 1981, at Gainesville, FL, under various water-limited treatments. Model simulations were compared with measured dry matter growth, LAI, specific leaf area, pod number, and pod mass over time during various time periods. Comparisons shown here are for illustration of water deficit effects, and are not meant to be a statement of model performance because the model was more or less calibrated to these data along with some 30 or 40 other seasons of soybean growth data at various locations.

One of our early experiments was conducted on 'Bragg' soybean sown at 30 plants m^{-2} on 15 June 1978, when the crop experienced a very severe terminal water deficit characterized by 53 d during which 16 mm of rainfall fell (or 61 d in which 33 mm rain fell). Experience with this experiment allowed us to calibrate

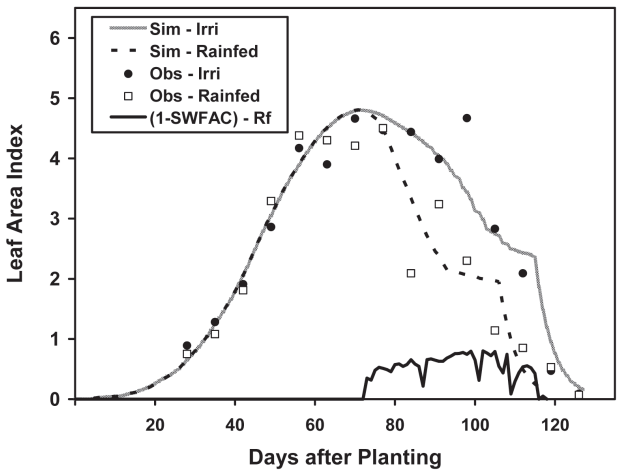

Fig. 3–23. Simulated LAI of rainfed and irrigated Bragg soybean in 1978 at Gainesville, FL. Also shown is (1-SWFAC) to illustrate severe water stress during the last half of the season (data from Wilkerson et al., 1983).

leaf area abscission under water deficit, as well as setting a sufficiently rapid and deep rooting profile to achieve the grain yield actually obtained under water-limited conditions (1178 compared with 3041 kg ha^{-1} for the irrigated crop). The simulated LAI (Fig. 3–23) distinctly shows the rapid leaf abscission that occurred during the water deficit period. The simulated shoot mass of the rainfed crop did not increase over the last 42 d of the season (Fig. 3–18). Nevertheless, pods were added after a delay and simulated pod and seed masses of 1498 and 1052 kg ha^{-1} were produced using stored water in the profile over that 53- to 61-d period, plus the small amount of rainfall (16–33 mm) that fell (Fig. 3–18).

In 1981, an experiment was conducted on 'Cobb' soybean sown at 36 plants m^{-2} in 76-cm rows on 26 June (Bovi, 1983). A treatment under rainfed conditions during vegetative growth experienced two short 8-d periods of water deficit that reduced dry matter accumulation over time (Fig. 3–24). The simulated specific leaf area (SLA) was reduced by the TURFAC stress factor (Fig. 3–25), although the decrease was not as great as the data suggested. The reduced SLA and reduced dry matter allocation caused reduced LAI (Fig. 3–26). The model generally simulated the dynamics of water stress on SLA, LAI, and biomass accumulation fairly well relative to these two 8-d water deficit periods. Insufficient water stress reductions of SLA, LAI, and biomass may be related to either too rapid early rooting or insufficient ET demand, the latter most likely associated with the underprediction of LAI at very early stages even for irrigated plants.

In 1984, an experiment was conducted on irrigated vs. rainfed 'Bragg' soybean sown on 12 June at Gainesville, FL (Maliro, 1986; DeVries et al., 1989a, 1989b). The rainfed treatment was exposed to a 28-d period (71–98 d after sowing) with just 14 mm of rainfall, which caused 12 d of simulated stress that was relieved by

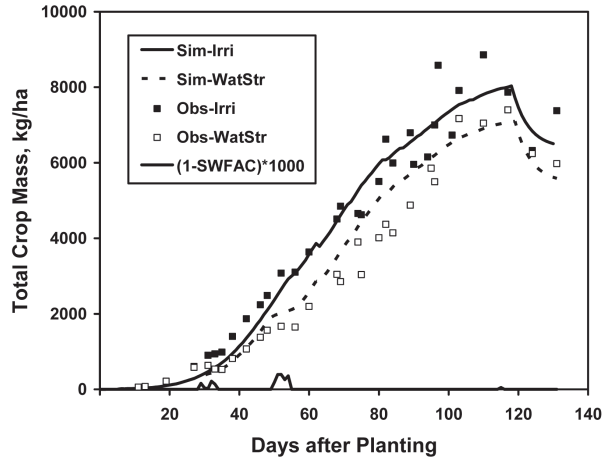

Fig. 3–24. Simulated crop biomass over time and (1-SWFAC) for a rainfed treatment that experienced two short 8-d periods of water deficit during vegetative growth compared with fully irrigated Cobb soybean grown at Gainesville, FL, in 1981. Data from Bovi (1983).

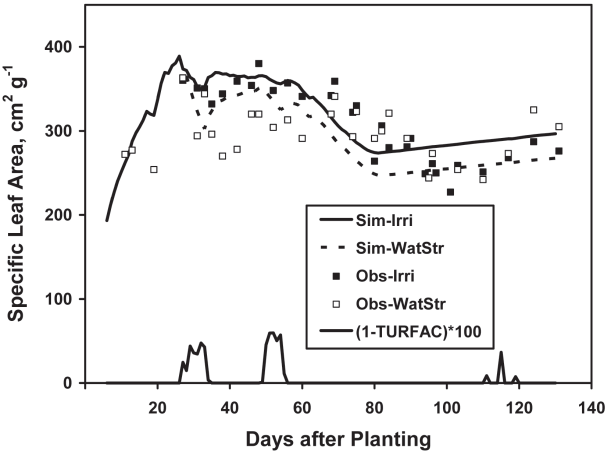

Fig. 3–25. Simulated specific leaf area and (1-TURFAC) over time for a rainfed treatment that experienced two short 8-d periods of water deficit during vegetative growth compared with fully irrigated Cobb soybean grown at Gainesville, FL, in 1981 (data from Bovi, 1983).

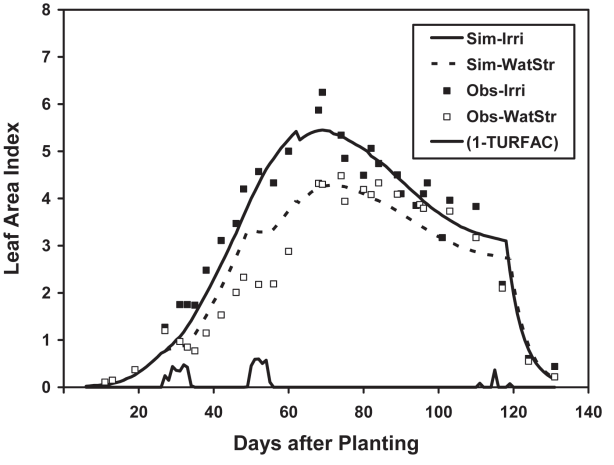

Fig. 3–26. Simulated LAI and (1-TURFAC) over time for a rainfed treatment that experienced two short 8-d periods of water deficit during vegetative growth compared with fully irrigated Cobb soybean grown at Gainesville, FL, in 1981 (data from Bovi, 1983).

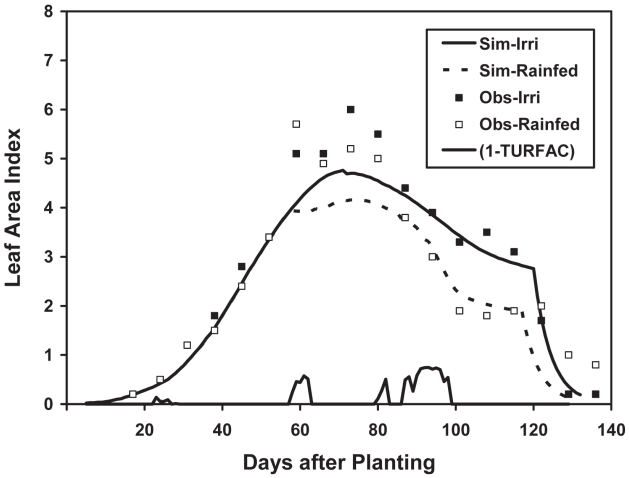

Fig. 3–27. Simulated LAI and (1-TURFAC) over time for rainfed and irrigated Bragg soybean grown on a Kendrick fine sand at Gainesville, FL, in 1984 (data from Maliro, 1986).

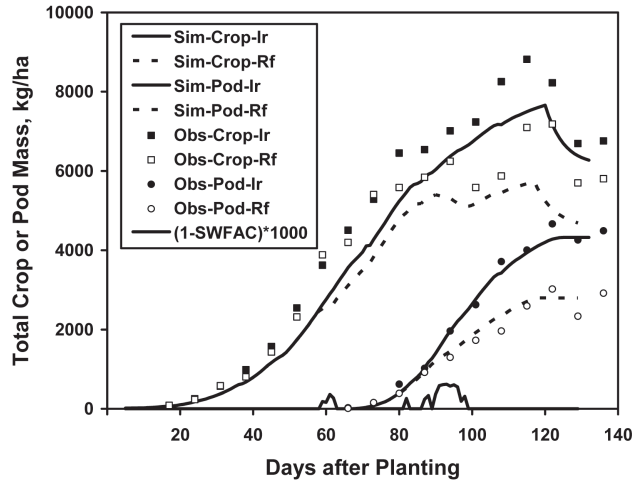

Fig. 3–28. Simulated total crop and pod mass and (1-SWFAC) over time for rainfed and irrigated Bragg soybean grown on a Kendrick fine sand at Gainesville, FL, in 1984 (data from Maliro, 1986).

irrigation on Day 99. The simulated water deficit (during 82–98 d) occurred during early reproductive growth when pods and seeds were just being added. The simulated and observed LAI were dramatically reduced during the water deficit period (Fig. 3–27). Dry matter accumulation in total crop and pod mass in the rainfed treatment were dramatically reduced starting at 80 d after sowing (Fig. 3–28). In this case, the predicted reduction in seed growth and yield was associated with a smaller number of seeds set during the water deficit period. The reduction in seed number carried by the plants (Fig. 3–29) was strictly caused by the reduction in canopy photosynthesis rate.

Observed mass per seed showed a slower single seed growth rate for the rainfed than the irrigated treatment for Bragg soybean grown in 1984 in Gainesville,

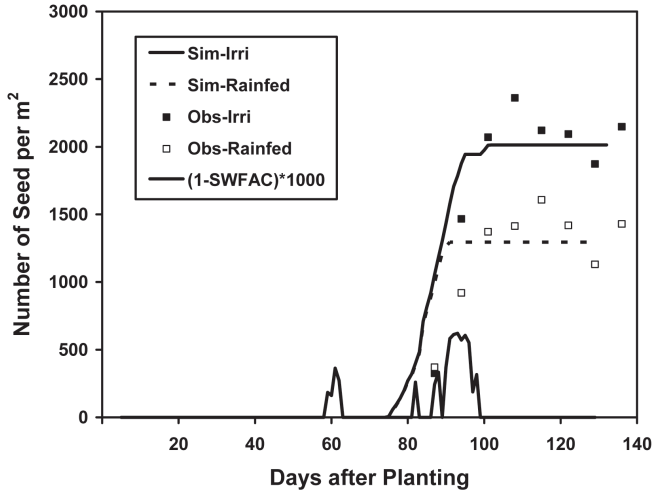

Fig. 3–29. Simulated seed number over time and (1-SWFAC) for rainfed and irrigated Bragg soybean grown on a Kendrick fine sand at Gainesville, FL, in 1984 (data from Maliro, 1986).

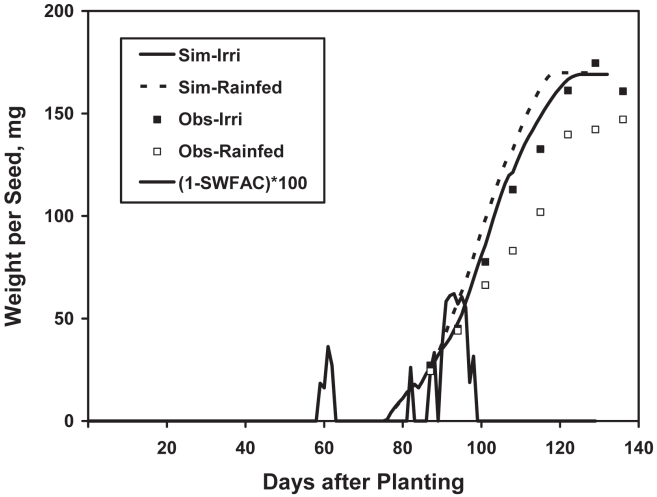

Fig. 3–30. Simulated mass per seed over time and (1-SWFAC) for rainfed and irrigated Bragg soybean grown on a Kendrick fine sand at Gainesville, FL, in 1984 (data from Maliro, 1986).

FL, but the simulations did not reproduce that response (Fig. 3–30). The same phenomena of failing to simulate the slower observed single seed growth rate under water deficit also occurred in the 1988 drought season compared with the 1990 rainy season for Williams 82 soybean grown in Ames, IA (data not shown). The point we wish to make here is that potential growth rate per seed (we think this is related to fewer number of cells from cell division) should be reduced as a consequence of water deficit and/or heat stress (associated with drought), such that the single seed growth rate remains depressed after the water deficit period is relieved. This feature will be incorporated into a future version of the model. An additional aspect related to this seed growth phenomenon could be that the rate (slope) of addition of pods (seeds) should be reduced somewhat more under

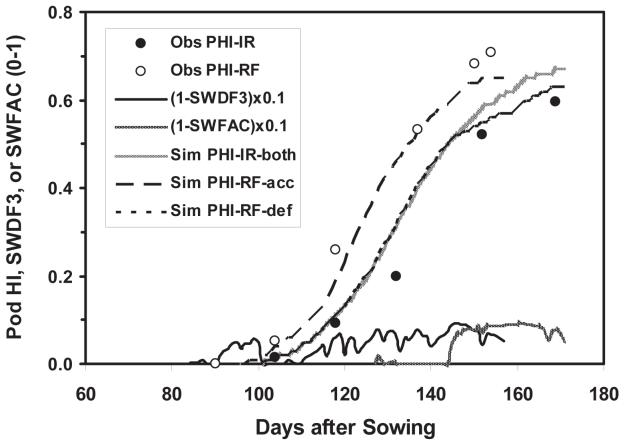

Fig. 3–31. Simulated and observed pod harvest index (PHI), (1-SWFAC), and (1-SWDF3) for rainfed and irrigated treatments of faba bean 'Alameda' grown in 1987–1988 season in Cordoba, Spain, with default (def) and acceleration (acc) versions of the model [data from Sau (1989) and Sau and Minguez (2000)].

water deficit although the final carrying capacity (seed load) is predicted adequately (Fig. 3–29).

Potential Improvements in Sensing of Soil Water: Evidence from a Faba Bean Drought Study

As discussed previously, CROPGRO V4.02 uses the SWFAC signal to delay or accelerate progression to reproductive stages using growth phase-specific modifiers. We frequently have observed that water deficit accelerates final maturity in soybean, dry bean, and faba bean, and the model currently predicts this reasonably well. However, there is strong acceleration of onset of reproductive growth (pod number, pod and seed mass, and pod harvest index) in chickpea and faba bean (Sau and Minguez, 2000), and to a lesser extent, in dry bean and soybean, and the current model V4.02 does not handle onset-acceleration well. The observed acceleration was dramatic in faba bean where onset of pod harvest index and pod mass was shifted 8 to 10 d earlier under water deficit in the 1987–1988 season at Cordoba, Spain (Fig. 3–31). This behavior could not be triggered with the SWFAC of the model (Boote et al., 2002), because that signal was 30 to 40 d late in signaling, even though the SWFAC correctly predicted when dry matter accumulation began to slow down in the rainfed treatment (Fig. 3–32). To solve the problem, we hypothesized a new signal, SWDF3, based on the ratio of TRWU/EP_O, but scaled to act much earlier (Eq. [23]).

$$SWDF3 = TRWU/(EP_O \times K_1) \quad [23]$$

$$PROG(J) = FT(J) \times FDL(J) \times [1 + (1 - SWDF3) \times WSENP(J)] \quad [24]$$

One can think of TRWU as typically being in excess capacity when most of the roots are in upper soil layers and those layers are wet. Based on trial and error,

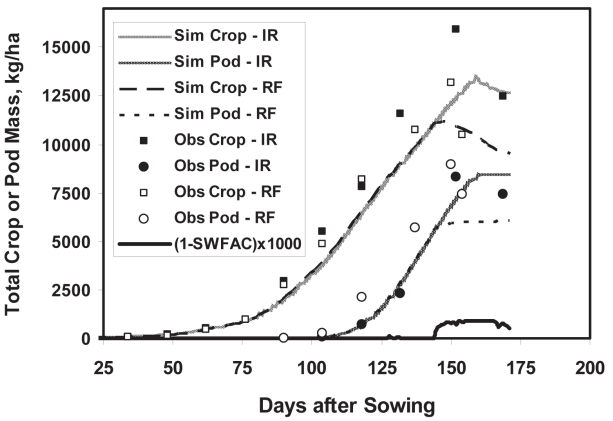

Fig. 3–32. Simulated and observed total crop mass, pod mass and (1-SWFAC) for rainfed and irrigated treatments of faba bean Almeda grown in 1987–1988 season in Cordoba, Spain, with the default CROPGRO-faba bean model [data from Sau (1989) and Sau and Minguez (2000)].

we found that when the ratio of TRWU to EP_O dropped below five (Fig. 3–33), we could use that as a successful early signal to accelerate timing of pod and seed cohorts, rate of pod addition, root depth progression, and maturity. This signal allowed the CROPGRO-Faba bean model to accelerate the onset timing of reproductive organs (PHI, Fig. 3–31; pods and seeds, Fig. 3–34) by as much as 8 to 10 d using Eq. [24], even while the crop dry matter accumulation continued unaffected. The rate of progress PROG(J) in Eq. [24] is a function of thermal effect FT(J), daylength effect FDL(J), and WSENP(J) that is a phase-dependent and species-dependent modifier. Model sensitivity analyses suggested that the same early signal also worked well to accelerate rate of pod addition, reduce leaf expansion (thicker leaves) and accelerate rooting front. Model code changes were also necessary to allow the signal to affect all subsequent cohorts rather than just the first cohort (stage), which is all the current model considers. For faba bean, the K_1 modifier to accelerate maturity had to be 3.0 rather than the 5.0 used to accelerate onset. The same early signal approach was attempted with the CROPGRO model for soybean and dry bean that were found to have some acceleration of reproductive sites under water deficit, but the K_1 modifier ratio had to be 2.5 for onset phenomena and smaller (1.5) for maturity. While there may be other complicating factors such as different soils and climates that affected our evaluation of these different species, we believe that species differ in sensitivity and the K_1 modifier on this ratio will need to be a "species" coefficient to be general. These code changes are being considered for a future version of the CROPGRO model to improve how it predicts delay or acceleration of the onset and rate of pod addition and reproductive processes, but caution is needed in applying to different species and different processes.

We actually believe that this early signal phenomenon is related to the abscisic acid signal observed when soil dries out in upper soil layers and signals to

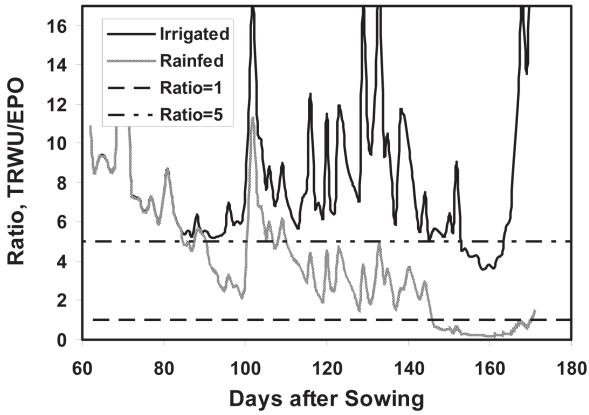

Fig. 3–33. Simulated ratio of potential root water uptake to transpirational demand (TRWU/EP) over time for rainfed and irrigated treatments of faba bean Almeda grown in 1987–1988 season in Cordoba, Spain. The thresholds of SWFAC (1.0) and the new signal SWDF3 (5.0) are shown.

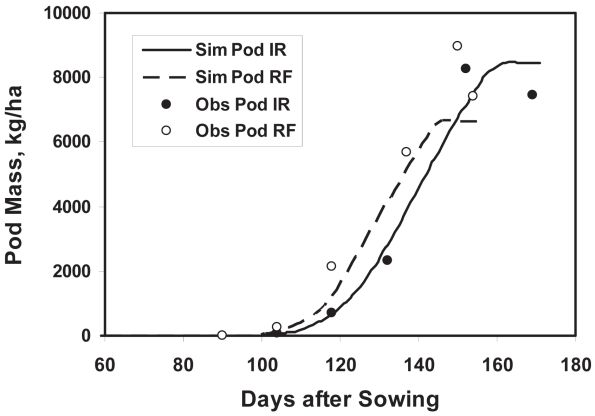

Fig. 3–34. Simulated and observed pod mass for rainfed and irrigated faba bean Almeda grown in 1987–1988 season in Cordoba, Spain, with acceleration version of the CROPGRO-faba bean model [data from Sau (1989) and Sau and Minguez (2000)].

reduce leaf expansion and reduce stomatal conductance despite not much reduction in plant water potential (Davies et al., 1990; Davies and Zhang, 1991; Tardieu et al., 1992). This proposed signal can be twofold stronger (earlier) than the TURFAC signal. In this particular study, specific leaf area was decreased rather early and stomatal conductance was increased slightly (Sau and Minguez, 2000) although crop dry matter accumulation and transpiration were not significantly reduced until much later (Fig. 3–32). This signal apparently accelerated reproductive timing of faba bean at an early stage when adequate water remained in the deep layers of the soil to maintain transpiration and photosynthesis, which was beneficial to increase yield under rainfed conditions because it allowed grain fill to start earlier at a time when photosynthate was still available (Fig. 3–32 and Fig. 3–34). This may be a trait that evolved genetically over time in this terminal drought situation of the Mediterranean climate.

Summary

We find that the Ritchie tipping bucket soil water balance model in DSSAT generally works satisfactorily, when the soil water holding traits (DUL, LL) are estimated properly for the soil in question and when root growth is adequately predicted. The RLD profile or root hospitality function, in our experience, distinctly does not have an "exponential decline" with depth. The prediction of the root depth front with time and proliferation with depth needs to be made more mechanistic in its response to soil traits both static and dynamic. The rooting front appears to be accelerated under water stress and roots appear to grow through drying soil layers so long as impedance is not a problem. There are four PET options used with CROPGRO of which three (FAO-24, FAO-56, and a prototype hourly energy balance) require additional inputs of windrun and dewpoint temperature. The FAO-56 PET option works well, but the FAO-24 overpredicts ET and soil water extraction. In our experience with CROPGRO V3.5 for faba bean and soybean (Sau et al., 2004) and with CERES-Maize V3.5 for maize (Lopez-Cedron et al., 2008), we found that the default Priestley-Taylor option is satisfactory if used with a lower extinction coefficient (KEP) for partitioning of PET to transpiration (EP) as a function of LAI. Otherwise, the models tended to overpredict ET, particularly early in the season, thus creating too much soil water extraction and too much water deficit in early season. This was solved by reducing the KEP from 0.85 to 0.70 for all CROPGRO V4.0 crops and from 1.00 to 0.68 for CERES Maize.

Where the soil water balance is adequately predicted, the crop water stress signals, SWFAC and TURFAC, appear to function adequately to modify crop assimilation and expansive growth processes as well as most crop phenological progressions. Sensitivity examples and comparisons to field data on soybean and other crops were given to show how these signals act to enhance partitioning to root, reduce SLA, reduce LAI, and accelerate crop maturity. Overall, CROPGRO satisfactorily simulates water deficit effects on growth and development processes, although improvements could be made to create crop-specific signals that act sooner than the current TURFAC to modify growth and phenology, especially the onset timing of reproductive growth.

References

Albrecht, S.L., J.M. Bennett, and K.J. Boote. 1984. Relationship of nitrogenase activity to plant water stress in field-grown soybeans. Field Crops Res. 8:61–71.

Allen, R.G., L.S. Pereira, D. Raes, and M. Smith. 1998. Crop evapotranspiration. Guidelines for computing crop water requirements. FAO Irrig. and Drainage Paper no. 56. FAO, Rome, Italy.

Boote, K.J., J.M. Bennett, J.W. Jones, and H.E. Jowers. 1989. On-farm testing of peanut and soybean models in North Florida. Paper no. 89040. ASAE, St. Joseph, MI.

Boote, K.J., and J.W. Jones. 1986. Applications of, and limitations to, crop growth simulation models to fit crops and cropping systems to semi-arid environments. p. 63–75. *In* F.R. Bidinger and

C. Johansen (ed.) Drought research priorities for the dryland tropics, Patancheru, India. 1986. Int. Crops Res. Inst. for the Semi-Arid Tropics, Patancheru, India.

Boote, K.J., J.W. Jones, W.D. Batchelor, E.D. Nafziger, and O. Myers. 2003. Genetic coefficients in the CROPGRO-soybean model: Links to field performance and genomics. Agron. J. 95:32–51.

Boote, K.J., J.W. Jones, and G. Hoogenboom. 1998a. Simulation of crop growth: CROPGRO model. p. 651–692. *In* R.M. Peart and R.B. Curry (ed.) Agricultural systems modeling and simulation. Marcel Dekker, New York.

Boote, K.J., J.W. Jones, G. Hoogenboom, W.D. Batchelor, and C.H. Porter. 2004. DSSAT v4 CROPGRO crop growth and partitioning module. p. 1–102. *In* J.W. Jones et al. (ed.) Decision support system for agrotechnology transfer Version 4.0, Vol. 4 DSSAT v4: Crop model documentation. Univ. of Hawaii, Honolulu, HI.

Boote, K.J., J.W. Jones, G. Hoogenboom, and N.B. Pickering. 1998b. The CROPGRO model for grain legumes. p. 99–128. *In* G.Y Tsuji et al. (ed.) Understanding options for agricultural production. Kluwer Academic Publ., Dordrecht.

Boote, K.J., M.I. Mínguez, and F. Sau. 2002. Adapting the CROPGRO legume model to simulate growth of faba bean. Agron. J. 94:743–756.

Boote, K.J., and N.B. Pickering. 1994. Modeling photosynthesis of row crop canopies. HortScience 29:1423–1434.

Boote, K.J., N.B. Pickering, and L.H. Allen, Jr. 1997. Plant modeling: Advances and gaps in our capability to project future crop growth and yield in response to global climate change. p. 179–228. *In* L.H. Allen, Jr., et al. (ed.) Advances in carbon dioxide effects research. ASA Spec. Publ. 61. ASA, CSSA, and SSSA, Madison, WI.

Boote, K.J., J.R. Stansell, A.M. Schubert, and J.F. Stone. 1983. Irrigation, water use, and water relations. p. 164–205. *In* H.E. Pattee and C.T. Young (ed.) Peanut science and technology. Am. Peanut Res. and Educ. Soc., Yoakum, TX.

Bovi, O.A. 1983. Estimating carbon balance of field-grown soybeans. Ph.D. diss. Univ of Florida, Gainesville.

Calmon, M.A., W.D. Batchelor, J.W. Jones, J.T. Ritchie, K.J. Boote, and L.C. Hammond. 1999. Simulating soybean root growth and soil water extraction using a functional crop model. Trans. ASAE 42:1867–1877.

Davies, W.J., T.A. Mansfield, and A.M. Hetherington. 1990. Sensing of soil water status and the regulation of plant growth and development. Plant Cell Environ. 13:709–720.

Davies, W.J., and J. Zhang. 1991. Root signals and the regulation of growth and development of plants in drying soil. Annu. Rev. Plant Physiol. 42:55–76.

Desclaux, D., and P. Roumet. 1996. Impact of drought stress on the phenology of two soybean (*Glycine max* L. Merr) cultivars. Field Crops Res. 46:61–70.

DeVries, J.D., J.M. Bennett, S.L. Albrecht, and K.J. Boote. 1989a. Water relations, nitrogenase activity, and root development of three grain legumes in response to soil water deficits. Field Crops Res. 21:215–226.

DeVries, J.D., J.M. Bennett, K.J. Boote, S.L. Albrecht, and C.E. Maliro. 1989b. Nitrogen accumulation and partitioning by three grain legumes in response to soil water deficits. Field Crops Res. 22:33–44.

Eitzinger, J., M. Trnka, J. Hosch, Z. Zalud, and M. Dubrovsky. 2004. Comparison of CERES, WOFOST and SWAP models in simulating soil water content during growing season under different soil conditions. Ecol. Model. 171:223–246.

Erbs, D.G., S.A. Klein, and J.A. Duffie. 1982. Estimation of the diffuse radiation fraction for hourly, daily and monthly-average global radiation. Sol. At. Energy 28:293–302.

Fisher, D.B. 2000. Phloem transport. p. 758–776. *In* B.B. Buchanan et al. (ed.) Biochemistry and molecular biology of plants. Am. Soc. Plant Physiol., Rockville, MD.

Gijsman, A.J., G. Hoogenboom, W.J. Parton, and P.C. Kerridge. 2002a. Modifying DSSAT crop models for low-input agricultural systems using a soil organic matter-residue module from CENTURY. Agron. J. 94:462–474.

Gijsman, A.J., S.S. Jagtap, and J.W. Jones. 2002b. Wading through a swamp of complete confusion: How to choose a method for estimating soil water retention parameters for crop models. Eur. J. Agron. 18:75–105.

Gijzen, H., and J. Goudriaan. 1989. A flexible and explanatory model of light distribution and photosynthesis in row crops. Agric. For. Meteorol. 48:1–20.

Gilbert, R.A., K.J. Boote, and J.M. Bennett. 2002. On-farm testing of the PNUTGRO crop growth model in Florida. Peanut Sci. 29:58–65.

Godwin, D.C., and D.C. Jones. 1991. Nitrogen dynamics in soil-plant systems. p. 287–321. *In* J. Hanks and J.T. Ritchie (ed.) Modeling plant and soil systems. Agron. Monogr. 31. ASA, CSSA, and SSA, Madison, WI.

Godwin, D.C., and U. Singh. 1998. Nitrogen balance and crop response to nitrogen in upland and lowland cropping systems. p. 55–77. *In* G.Y. Tsuji et al. (ed.) Understanding options for agricultural production. System approaches for sustainable agricultural development. Kluwer Academic Publ., Dordrecht, the Netherlands.

Goudriaan, J. 1977. Crop micrometeorology: A simulation study. Simulation monographs. Pudoc, Wageningen, the Netherlands.

Goudriaan, J., and H.H. Van Laar. 1994. Modelling potential crop growth processes. Textbook with exercises. Kluwer Academic Publ., Dordrecht, the Netherlands.

Hoogenboom, G., J.W. Jones, and K.J. Boote. 1991. Predicting growth and development with a generic grain legume model. Paper no. 91–4501. ASAE, St. Joseph, MI.

Hoogenboom, G., J.W. Jones, and K.J. Boote. 1992. Modeling growth, development, and yield of grain legumes using SOYGRO, PNUTGRO, and BEANGRO: A review. Trans. ASAE 35:2043–2056.

Hoogenboom, G., J.W. Jones, K.J. Boote, W.T. Bowen, N.B. Pickering, and W.D. Batchelor. 1993. Advancement in modeling grain legume crops. Paper no. 93–4511. ASAE, St. Joseph, MI.

Hoogenboom, G., J.W. Jones, P.W. Wilkens, W.D. Batchelor, W.T. Bowen, L.A. Hunt, N.B. Pickering, U. Singh, D.C. Godwin, B. Baer, K.J. Boote, J.T. Ritchie, and J.W. White. 1994. Crop models. p. 95–244. *In* G.Y. Tsuji et al. (ed.) DSSAT Version 3. Vol. 2. Univ. of Hawaii, Honolulu, HI.

Jagtap, S.S., and J.W. Jones. 1989. Evapotranspiration model for developing crops. Trans. ASAE 32:1342–1350.

Jensen, M.E., R.D. Burmaan, and R.G. Allen (ed.) 1990. Evapotranspiration and irrigation water requirements: A manual. Am. Soc. of Civil Engineers, New York.

Jones, C.A., W.L. Bland, J.T. Ritchie, and J.R. Williams. 1991. Simulation of root growth. p. 91–123. *In* J. Hanks and J. T. Ritchie (ed.) Modeling plant and soil systems. Agron. Monogr. 31. ASA, CSSA, and SSSA, Madison, WI.

Jones, J.W., K.J. Boote, G. Hoogenboom, J. White, and C.H. Porter. 2004. Phenology sub-module for CROPGRO. p. 1–21. *In* J.W. Jones et al. (ed.) Decision support system for agrotechnology transfer Version 4.0, Vol. 4 DSSAT v4: Crop model documentation. Univ. of Hawaii, Honolulu, HI.

Jones, J.W., G. Hoogenboom, C.H. Porter, K.J. Boote, W.D. Batchelor, L.A. Hunt, P.W. Wilkens, U. Singh, A.J. Gijsman, and J.T. Ritchie. 2003. DSSAT cropping system model. Eur. J. Agron. 18:235–265.

Kimball, B.A., and L.A. Bellamy. 1986. Generation of diurnal solar radiation, temperature, and humidity patterns. Energy Agric. 5:185–197.

Lopez-Cedron, F.X., K.J. Boote, J. Pineiro, and F. Sau. 2008. Improving the CERES-Maize model ability to simulate water deficit effects on maize production and yield components. Agron. J. 100:296–307.

Maliro, C.E. 1986. Physiological aspects of yield among four legume crops under two water regimes. M.S. thesis. Univ of Florida, Gainesville.

Naab, J.B., P. Singh, K.J. Boote, J.W. Jones, and K.O. Marfo. 2004. Using the CROPGRO-peanut model to quantify yield gaps of peanut in the Guinean savanna zone of Ghana. Agron. J. 96:1231–1242.

Mason, W.K., H.M. Taylor, A.T.P. Bennie, H.R. Rowse, D.C. Reicosky, Y. Jung, A.A. Righs, R.L. Yang, T.C. Kaspar, and J.A. Stone. 1980. Soybean row spacing and soil water supply. USDA Publ. AAT-NC-5. USDA ARS, Peoria, Illinois.

Nielsen, D.C., L. Ma, L.R. Ahuja, and G. Hoogenboom. 2002. Simulating soybean water stress effects with RZWQM and CROPGRO models. Agron. J. 94:1234–1243.

Parton, W.J., and J.A. Logan. 1981. A model for diurnal variation in soil and air temperature. Agric. For. Meteorol. 23:205–216.

Pickering, N.B., J.W. Jones, and K.J. Boote. 1995. Adapting SOYGRO V5.42 for prediction under climate change conditions. p. 77–98. *In* C. Rosenzweig et al. (ed.) Climate change and agriculture: Analysis of potential international impacts. ASA Spec. Publ. 59. ASA, CSSA, and SSSA, Madison, WI.

Pickering, N.B., J.W. Jones, and K.J. Boote. 1990. A moisture- and CO_2-sensitive model for evapotranspiration and photosynthesis. Paper no. 90-2519. ASAE, St. Joseph, MI.

Priestley, C.H.B., and R.J. Taylor. 1972. On the assessment of surface heat and evaporation using large scale parameters. Mon. Weather Rev. 100:81–92.

Porter, C.H., J.W. Jones, G. Hoogenboom, P.W. Wilkens, J.T. Ritchie, N.B. Pickering, K.J. Boote, and B. Baer. 2004. DSSAT v4 soil water balance module. p. 1–23. *In* J.W. Jones et al. (ed.) Decision support system for agrotechnology transfer Version 4.0, Vol. 4 DSSAT v4: Crop model documentation. Univ. of Hawaii, Honolulu, HI.

Ritchie, J.T. 1972. Model for predicting evaporation from a row crop with incomplete cover. Water Resour. Res. 8:1204–1213.

Ritchie, J.T. 1985. A user–oriented model of the soil water balance in wheat. p. 293–305. *In* E. Fry and T.K. Atkin (ed.) Wheat growth and modeling. NATO-ASI Series, Plenum Press.

Ritchie, J.T. 1998. Soil water balance and plant water stress. p. 41–54. *In* G.Y. Tsuji et al. (ed.) Understanding options for agricultural production. Kluwer Academic Publ., Dordrecht, The Netherlands.

Robertson, W.K., L.C. Hammond, J.T. Johnson, and K.J. Boote. 1980. Effects of plant-water stress on root distribution of corn, soybeans, and peanuts in sandy soil. Agron. J. 72:548–550.

Ruíz-Nogueira, B., K.J. Boote, and F. Sau. 2001. Calibration and use of CROPGRO-soybean model for improving soybean management under rainfed conditions. Agric. Syst. 68:151–173.

Sau, F. 1989. Influencia de la nutricion nitrogenada sobre la respuesta al deficit hidrico en soja y habas. Doctoral diss. Servicio de Publicaciones de la Universidad de Cordoba.

Sau, F., K.J. Boote, W.M. Bostick, J.W. Jones, and M.I. Minguez. 2004. Testing and improving evapotranspiration and soil water balance of the DSSAT crop models. Agron. J. 96:1243–1257.

Sau, F., and M.I. Minguez. 2000. Adaptation of indeterminate faba bean to weather and management under a Mediterranean Climate. Field Crops Res. 66:81–99.

Saxton, K.E., W.J. Rawls, J.S. Romberger, and R.I. Papendick. 1986. Estimating generalized soil–water characteristics from texture. Soil Sci. Soc. Am. J. 50:1031–1036.

Singh, P., K.J. Boote, A.Y. Rao, M.R. Iruthayaraj, A.M. Sheikh, S.S. Hundal, R.S. Narang, and P. Singh. 1994. Evaluation of the groundnut model PNUTGRO for crop response to water availability, sowing dates, and seasons. Field Crop Res. 39:147–162.

Spitters, C.J.T., H.A.J.M. Toussaint, and J. Goudriaan. 1986. Separating the diffuse and direct components of global radiation and its implications for modeling canopy photosynthesis: I. Components of incoming radiation. Agric. For. Meteorol. 38:217–229.

Sprent, J.I. 1972. The effects of water stress on nitrogen-fixing root nodules: IV. Effects on whole plants of *Vicia faba* and *Glycine max*. New Phytol. 71:603–611.

Tardieu, F., J. Zhang, N. Katerji, O. Bethenod, S. Palmer, and W.J. Davies. 1992. Xylem ABA controls the stomatal conductance of field-grown maize subjected to soil compaction or soil drying. Plant Cell Environ. 15:193–197.

Villalobos, F.J., and E. Fereres. 1990. Evaporation measurements beneath corn, cotton, and sunflower canopies. Agron. J. 82:1153–1159.

Wilkerson, G.G., J.W. Jones, K.J. Boote, K.T. Ingram, and J.W. Mishoe. 1983. Modeling soybean growth for crop management. Trans. ASAE 26:63–73.

Williams, J.H., and K.J. Boote. 1995. Physiology and modelling—Predicting the "Unpredictable Legume". p. 301–353. *In* H.E. Pattee and H.T. Stalker (ed.) Advances in peanut science. Am. Peanut Res. and Educ. Soc., Stillwater, OK.